Cellular and Molecular Life Sciences (2025) 82:136
https://doi.org/10.1007/s00018-025-05672-2

ORIGINAL ARTICLE

Siglec-15 is a putative receptor for porcine epidemic diarrhea virus infection

Zhihua Feng[1,2,3,4] · Yajuan Fu[3,4] · Sheng Yang[3,4] · Heng Zhao[3,4] · Minhua Lin[3,4] · Chuancheng Liu[3,4] · Weili Huang[3,4] · Xinyan He[3,4] · Yao Chen[3,4] · Jianxin Chen[1,2] · Yangkun Shen[3,4] · Zhaolong Li[5] · Qi Chen[1,2,3,4]

Received: 1 February 2025 / Revised: 14 March 2025 / Accepted: 18 March 2025
© The Author(s) 2025

Abstract

Porcine epidemic diarrhea virus (PEDV) has caused significant losses in the pork industry, but the mechanism of PEDV infection is still unclear. On the basis of our RNA-Seq data and due to the potential role of sialic acid as a coreceptor, we investigated the function of sialic acid-binding Ig-like lectin 15 (Siglec-15) to determine its role as a receptor in PEDV infection. We found that Siglec-15 enhances PEDV infection by promoting viral adsorption to host cells. Coimmunoprecipitation and immunofluorescence assays revealed that Siglec-15 binds to the S1 subunit and M protein of PEDV. PEDV infectivity was significantly reduced in Siglec-15 knockout mice. In addition, we developed a monoclonal antibody targeting Siglec-15 that can effectively inhibit PEDV infection both in vitro and in vivo. Overall, our study suggests that Siglec-15 may be a receptor for PEDV infection, which is important for related mechanistic studies and reveals a novel target for anti-PEDV therapeutic development.

Keywords Swine alpha-coronaviruses · Host factor · Mouse model · Antibody drug · Cross-species transmission

Introduction

Porcine epidemic diarrhea (PED) is an acute and highly contagious intestinal disease caused by the porcine epidemic diarrhea virus (PEDV) [1, 2]. PEDV infects pigs of all ages, with primary symptoms including severe diarrhea, vomiting, dehydration, enteritis, and weight loss [3]. Infection with PEDV is often fatal for suckling piglets, with mortality rates approaching 100% [4, 5]. PEDV was first identified in the United Kingdom in the 1970s, followed by reports of similar diseases in various European countries [6, 7]. The virus was first documented in Asia in the 1980s, but it did not attract significant attention until recently [8]. New large-scale PEDV outbreaks began in the winter of 2010, originating from pig farms in southern China and rapidly spreading across the country [4, 9]. This outbreak resulted in the death of more than one million piglets in southern China, with mortality rates ranging from 80 to 100%, causing catastrophic damage to the pork industry [4, 10]. Since 2013, PEDV has also been reported in the United States, Canada, Mexico, Peru, Germany, Belgium, Ukraine, France, Italy, and Austria [11–15]. Recent outbreaks have been attributed to virulent strains of PEDV, which exhibit multiple mutations in the S gene [16–18]. Phylogenetic analysis of the S

Zhihua Feng and Yajuan Fu contributed equally to this work and shared first authorship.

✉ Yangkun Shen
shenyk@fjnu.edu.cn

✉ Zhaolong Li
lizhao-long522@163.com

✉ Qi Chen
chenqi@fjnu.edu.cn

1 Key Laboratory of OptoElectronic Science and Technology for Medicine of Ministry of Education, Fujian Normal University, Fuzhou, Fujian 350117, China

2 College of Photonic and Electronic Engineering, Fujian Normal University, Fuzhou, Fujian 350117, China

3 Fujian Key Laboratory of Innate Immune Biology, Biomedical Research Center of South China, Fujian Normal University Qishan Campus, Fuzhou, Fujian Province 350117, China

4 College of Life Science, Fujian Normal University Qishan Campus, Fuzhou, Fujian Province 350117, China

5 Institute of Animal Husbandry and Veterinary Medicine, Fujian Academy of Agricultural Sciences, Fuzhou, Fujian Province 350013, China

Published online: 02 April 2025

gene indicates that PEDV can be classified into the G I and G II genotypes [18, 19], with the currently prevalent strains primarily belonging to the G II genotype.

PEDV is an enveloped, single-stranded, positive-sense RNA virus belonging to the genus *Alphacoronavirus* within the family *Coronaviridae*, with a genome approximately 28 kb in length [20, 21]. The PEDV genome comprises at least seven open reading frames (ORFs) that encode four structural proteins and 17 nonstructural proteins [22]. From 5' to 3', the genome consists of ORF 1a, ORF 1b, the spike protein (S), the helper protein ORF3, the envelope protein (E), the membrane protein (M), and the nucleocapsid protein (N) [23]. The S protein is a glycoprotein of approximately 150–220 kDa located on the virus surface that is characterized by genetic diversity, and plays a crucial role in mediating viral adsorption and entry and the induction of neutralizing antibody production in vivo, as well as influencing viral virulence [24, 25]. The spike protein can be cleaved by trypsin-like proteases into two subunits, S1 and S2. The S1 subunit can be further divided into the N-terminal domain (NTD, 19–252 aa) and the C-terminal domain (CTD, 509–638 aa) [26]. The NTD contains a sialic acid-binding region, which typically determines the tissue tropism of PEDV [27]. The CTD houses the receptor-binding domain (RBD), and the S1 subunit is also involved in the apoptosis of target cells induced by PEDV [28]. The S2 subunit primarily facilitates the fusion of PEDV with target cell membranes and the assembly of S protein trimers [29].

The M gene is 681 nucleotides in length and encodes a protein of approximately 27–32 kDa, classified as a type III glycoprotein [30, 31]. It consists of a short amino-terminal extracellular domain, three continuous transmembrane domains, and a long carboxy-terminal envelope domain [31]. The M protein is widely distributed throughout the cytoplasm and interacts with the spike protein (S) and nucleocapsid protein (N) during viral assembly. As the most abundant component of the viral envelope, the M protein plays a crucial role in virus assembly and budding, inhibits innate immune responses by blocking type I and type III interferon pathways, and induces protective antibodies in pigs [32].

Coronavirus infection of host cells is typically mediated by the binding of the spike (S) protein to cell surface receptors. Studies have demonstrated that traditional coronavirus receptors, such as aminopeptidase N (APN, CD13), angiotensin-converting enzyme 2 (ACE2), dipeptidyl peptidase-4 (DPP4), and human carcinoembryonic antigen-related cell adhesion molecule 1 (CEACAM1), are not receptors for PEDV [33, 34]. Although occludin and transferrin receptor 1 (TfR1) have been demonstrated to be involved in PEDV infection [35, 36], they do not participate directly in the binding of PEDV to target cells but rather assist in endocytosis during PEDV entry [35, 36]. In addition, SLC35A1 does not directly interact with PEDV particles but can facilitate PEDV adhesion by regulating the expression of ADAM17 [37]. Other identified host factors involved in PEDV infection include Follistatin-like protein 1 (FSTL1), Toll-like receptor 4 (TLR4), death receptor DR5, and CCR4-NOT complex subunit 2 (CNOT2). Specifically, FSTL1 facilitates PEDV internalization and attachment by enhancing TLR4 recognition of PEDV N and S proteins, thereby inducing viral adsorption to host cells [38]. DR5 contributes to PEDV adsorption and internalization and promotes PEDV replication by modulating Caspase-8-dependent apoptosis; knockdown of DR5 significantly reduces PEDV-induced apoptosis [39]. Finally, CCR4-NOT complex subunit 2 (CNOT2) interacts with PEDV S protein, and CNOT2 knockout significantly inhibits PEDV replication in vitro [40]. The S protein of PEDV can bind to sialylated glycans, with Neu5Ac identified as the sugar type exhibiting the highest binding affinity in glycan array screenings, indicating that sialylated glycans may act as coreceptors for PEDV [26, 41].

Sialic acids (SAs) are a family of nine-carbon sugars that exist in two forms: free and bound. They are widely distributed across various organs and tissues [42]. Sialic acid can bind to a range of proteins, including selectins [43], factor H [44], sialic acid-binding Ig-like lectins (Siglecs) [45], L1 cell adhesion molecules (L1CAM) [46], uterine lectins [47], sperm sialic acid recognition proteins, and CD83 [48]. Siglecs are type I membrane proteins that recognize ubiquitous sialic acid epitopes on glycoconjugates within the cellular glycocalyx, transducing signals to regulate immune and inflammatory responses [49]. To date, 14 human Siglecs and 9 mouse Siglecs have been identified. Phylogenetically, the Siglec family can be divided into two groups: (i) Siglecs that are conserved across species but exhibit low sequence identity, including Siglec-1, Siglec-2, Siglec-4, and Siglec-15; and (ii) CD33-related Siglecs (CD33rSiglecs), which include Siglec-3, Siglec-5, Siglec-6, Siglec-7, Siglec-8, Siglec-9, Siglec-10, Siglec-11, Siglec-14, and Siglec-16 in humans [50].

Most Siglecs possess a variable amino-terminal domain (V-set) that binds sialic acid, as well as a variable number of C2 domains (C2-set), which are structurally similar to the variable and constant regions of antibodies, respectively [49]. Pathogens can employ Siglecs as receptors to facilitate host infection. For example, Siglec-1 and Siglec-10 mediate the cellular adsorption and endocytosis of porcine reproductive and respiratory syndrome virus (PRRSV) [51, 52]. Murine leukemia viruses (MLVs) utilize the interaction between their sialylated gangliosides and Siglec-1 to mediate infection and transmission [53]. Additionally, the expression level of Siglec-1 is correlated with the HIV-1

viral load, with the HIV-1 gp120 protein serving as a viral ligand for Siglec-1 and several CD33rSiglecs (Siglec-3, Siglec-5, Siglec-7, and Siglec-9) [54]. This interaction between Siglecs and gp120 promotes HIV infection in macrophages and T cells [55].

Siglec-15 is expressed primarily in macrophages and dendritic cells within the spleen and lymph nodes [56]. It consists of two immunoglobulin (Ig)-like domains, a transmembrane domain containing lysine residues, and a short cytoplasmic tail [56]. Siglec-15 plays a crucial role in regulating osteoclast maturation and bone remodeling by binding to lysine residues in its transmembrane domain, which activates the adaptor proteins DNAX-activating proteins DAP12 and DAP10, triggering downstream signaling cascades [57]. In the context of pathogenic microorganism infections, Siglec-15 has been implicated in the regulation of inflammatory responses induced by candida infection [58]. Additionally, Siglecs are closely associated with the occurrence and progression of various cancers and are emerging as important immune checkpoints for cancer therapy [59, 60]. However, the association of Siglec-15 with viral infections has not been reported.

In this study, we elucidated the mechanism by which Siglec-15 promotes PEDV infection. We further developed a monoclonal antibody targeting Siglec-15 and assessed its efficacy in blocking PEDV infection both in vitro and in vivo. These findings offer valuable insights into the infection mechanisms of PEDV, potential treatments for PEDV infection, and the development of resistant varieties.

Results

Effects of Sialic acid and its binding protein Siglec-15 on PEDV infection

N-acetylneuraminic acid (Neu5Ac) acts as a coreceptor for PEDV by binding to the S protein. Consequently, the addition of sialic acid or sialidase may influence PEDV infection of cells. To investigate the role of sialic acid in PEDV infection, we administered sialic acid concurrently with PEDV infection. Our data revealed that adding sialic acid (at concentrations of 1 mM, 0.5 mM, and 0.25 mM) to the culture medium significantly inhibited PEDV infection in 293T cells (Fig. 1A-C). Conversely, the introduction of sialidase (0.01 U, 0.02 U, 0.03 U, or 0.04 U) enhanced PEDV infection (Fig. 1D-F), suggesting that sialic acid on the cell surface may impede PEDV infection. Moreover, our results showd that the addition of sialic acid reduced PEDV binding to cells (Fig. 1G-I), confirming its role in the binding process. Interestingly, the cells treated with sialidase presented increased PEDV binding (Fig. 1G-I). These data suggest that although sialic acid on the cell surface is involved in the binding process of PEDV to cells, it may act as a critical factor that hinders effective PEDV adsorption.

To explore the role of sialic acid in PEDV infection, we hypothesized that sialic acid might effectively mask sialic acid-binding proteins by interacting with them on the cell surface, while treatments with sialidase may expose these sialic acid-binding proteins to enhance PEDV infection (Fig. 2A). To test this hypothesis, we analyzed the expression of sialic acid-binding proteins in 293T cells via RNA sequencing. Notably, we detected high expression levels of SEL-L (CD62L), CD83, L1CAM, Siglec-2, Siglec-3, Siglec-10, Siglec-15, Siglec-16, and CD24 (Fig. 2B). We then overexpressed these proteins in 293T cells and subsequently infected them with PEDV. Our findings indicated that overexpression of Siglec-15 significantly enhanced PEDV infection (Fig. 2C-D). These data suggest that Siglec-15 may play an important role in the infection process of PEDV.

Siglec-15 influences the adsorption of PEDV to cells but does not affect its internalization

To investigate the role of Siglec-15 in PEDV infection, we generated Siglec-15 knockout cell lines from 293T, L929, and LLC-PK1 cells. The results demonstrated that the ability of $293T^{Siglec-15-/-}$, $L929^{Siglec-15-/-}$, and LLC-$PK1^{Siglec-15-/-}$ cells to support PEDV infection was significantly reduced compared with that of wild-type cells (Fig. 3A-J; Supplementary Fig. 1). However, reintroduction of Siglec-15 restored the capacity for PEDV infection (Fig. 3A-J), confirming its involvement in the infection process. Coronavirus infection can involve multiple steps, including adsorption, entry, uncoating, genome replication and transcription, protein synthesis and assembly, and virus budding and release. Given that members of the Siglec family are known to facilitate viral adsorption and internalization, we specifically examined the effects of Siglec-15 knockout on these processes in LLC-PK1 cells. Our findings revealed that the knockout of *Siglec-15* significantly decreased PEDV adsorption, whereas PEDV internalization remained unaffected (Fig. 3K-L; Supplementary Fig. 2). Furthermore, PEDV adsorption was inhibited in LLC-$PK1^{Siglec-15-/-}$ cells, regardless of whether the virus or cells were pretreated with sialic acid or sialidase (Fig. 3M). In contrast, treatment of wild-type cells with sialidase enhanced PEDV infection by promoting viral adsorption through exposure to Siglec-15. Interestingly, the knockout of Siglec-15 did not eliminate PEDV infection, suggesting that Siglec-15 is not the sole factor responsible for mediating PEDV infection.

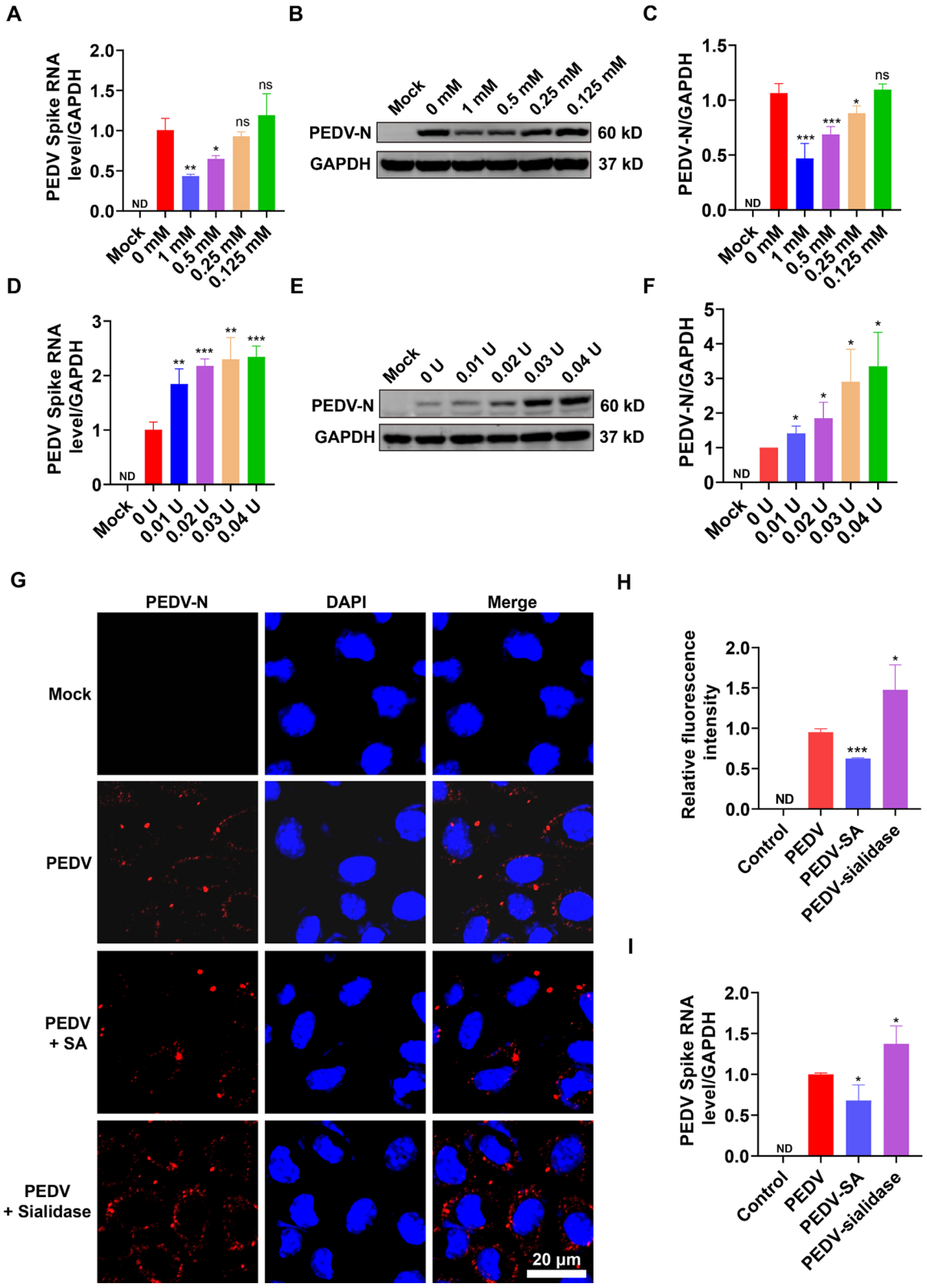

PEDV viral particles interact with Siglec-15 through the S and M proteins

The viral adsorption process during coronavirus infection is typically mediated by the binding of the spike (S) protein to receptors on the cell surface. Therefore, we further

Fig. 1 Sialic acid inhibits, but sialidase enhances PEDV infection. (**A-B**) The effects of various concentrations of sialic acid on PEDV infection (1 TCID50 per cell, 36 h post-infection) were assessed via RT-qPCR and Western blotting ($n=3$). (**C**) The expression of the PEDV N protein in **B** was quantified via ImageJ. (**D-E**) RT-qPCR and Western blotting were employed to evaluate the impact of different units of sialidase on PEDV infection (0.2 TCID50 per cell, 36 h post-infection) ($n=3$). (**F**) The expression of the PEDV N protein in **E** was quantified with ImageJ. (**G**) An immunofluorescence assay was conducted to examine the effects of sialic acid (1 mM) and sialidase (0.04 U) on PEDV adsorption (50 TCID50 per cell, maintained at 4 °C for 2 h) ($n=3$). (**H**) The content of the PEDV N protein in **G** was quantified via ImageJ. (**I**) RT-qPCR was utilized to assess the effects of sialic acid (1 mM) and sialidase (0.04 U) on PEDV adsorption (10 TCID50 per cell, maintained at 4 °C for 2 h) ($n=3$). The data are expressed as the means ± standard deviations and were analyzed via unpaired *t*-tests. $*P<0.05$, $**P<0.01$, and $****P<0.0001$. The scale bar in *G* indicates 20 μm

investigated the interaction characteristics of Siglec-15 with PEDV structural proteins. Coimmunoprecipitation data revealed that human, porcine, and mouse Siglec-15 could all bind to PEDV viral particles (Fig. 4A-C). Further immunofluorescence analyses revealed that Siglec-15 from these species colocalizes with the PEDV S1 and M proteins but not with the S2, E, or N proteins (Fig. 4D-K; Supplementary Fig. 3A-C). Additionally, the coimmunoprecipitation results confirmed the binding of human, porcine, and mouse Siglec-15 to the PEDV S1 subunit and M protein (Fig. 4L-Q). 3D structure prediction via AlphaFold 3 and molecular docking analyses indicated that Siglec-15 interacts with both the S1 subunit and the M protein of PEDV (Fig. 5A-B). Notably, both the V domain and the C2 domain are involved in the binding of Siglec-15 to the S1 subunit, whereas only the V domain participates in binding to the M protein (Fig. 5A-B). The predicted surface interface areas for the complexes of porcine Siglec-15 with the S and M proteins were 828.4 Å² and 840.8 Å², respectively, with binding free energies (ΔiG) of −62.2 kcal/mol and −1.5 kcal/mol, respectively. The entropy changes after dissociation (TΔS) were 13.4 kcal/mol and 12.7 kcal/mol, respectively.

To validate these predictions, we utilized porcine Siglec-15 variants: one with a deletion of the N-terminal random coil and V domain (P-S15ΔNRC-V), another with a deletion of the N-terminal random coil and C2 domain (P-S15ΔNRC-C2), and a variant with deletions of both the V and C2 domains (P-S15ΔV-C2). These constructs were coexpressed with the S1 subunit or M protein in 293T cells (Fig. 5C-I, Supplementary Fig. 4). The immunofluorescence results revealed that both P-S15ΔNRC-V and P-S15ΔNRC-C2 were capable of colocalizing with the S1 subunit and M protein (Fig. 5D-I). In contrast, P-S15ΔV-C2 did not colocalize with either protein (Supplementary Fig. 4). Coimmunoprecipitation experiments further confirmed that both P-S15ΔNRC-V and P-S15ΔNRC-C2 interact with the PEDV S1 subunit and M protein (Fig. 5J-M). Therefore, we propose that Siglec-15 functions as a receptor for PEDV and facilitates viral infection by interacting with the S and M proteins.

Knockout of Siglec-15 significantly reduced PEDV infection in mice

To further investigate the role of Siglec-15 in PEDV infection in vivo, we used Siglec-15 knockout mice as an infection model. We found that Siglec-15 was predominantly expressed in the spleen, lung, and small intestine of the mice (Fig. 6A). The main organs infected by PEDV also presented high levels of Siglec-15 expression (Fig. 6B). RT-qPCR and immunohistochemical analyses revealed that knockout of Siglec-15 significantly inhibited PEDV infection in the spleen, lung, and small intestine of the mice (Fig. 6B-E). Therefore, the in vivo expression of Siglec-15 is critical for determining the distribution of PEDV infection. Furthermore, the absence of Siglec-15 markedly alleviated the alveolar wall thickening, small intestinal villus atrophy, and epithelial cell shedding associated with PEDV infection (Fig. 6F-G). Interestingly, while PEDV was capable of infecting the spleen, no significant histopathological changes were observed in the spleens of either wild-type or *Siglec-15* knockout mice (Fig. 6H). These data suggest that knockout of Siglec-15 could be a potential target for breeding new pig varieties resistant to PEDV infection.

The Siglec-15 monoclonal antibody effectively inhibited PEDV infection

We transfected an overexpression plasmid (Fig. 7A) encoding the extracellular region of human Siglec-15 (20–263 aa)-Fc into Expi293F cells and purified the H-Siglec-15 (20–263 aa)-Fc protein (Fig. 7B-C) from the culture medium via Protein A Resin FF. Since H-Siglec-15 (20–263 aa)-Fc contains TEV protease cleavage sites between the H-Siglec-15 and Fc regions, the Fc fragment needed to be excised to obtain the H-Siglec-15 (20–263 aa) fragment. To achieve this goal, we transformed a plasmid expressing the TEV protease into *Escherichia coli* BL21 and purified the TEV protease (Fig. 7D). Finally, we obtained the H-Siglec-15 (20–263 aa) protein through digestion with the TEV protease (Fig. 7E-F). Next, we immunized New Zealand rabbits with H-Siglec-15 (20–263 aa), extracted B-cell RNA, and obtained the light and heavy chains variable regions (VH and VL) of the Siglec-15 antibody via nested PCR following reverse transcription (Supplementary Fig. 5). 3D prediction results revealed that the VH and VL domains of the monoclonal Siglec-15 antibody could bind to Siglec-15 (Fig. 8A-B). The predicted surface interface area for the complex between Siglec-15 and the antibody was 951.2 Å²,

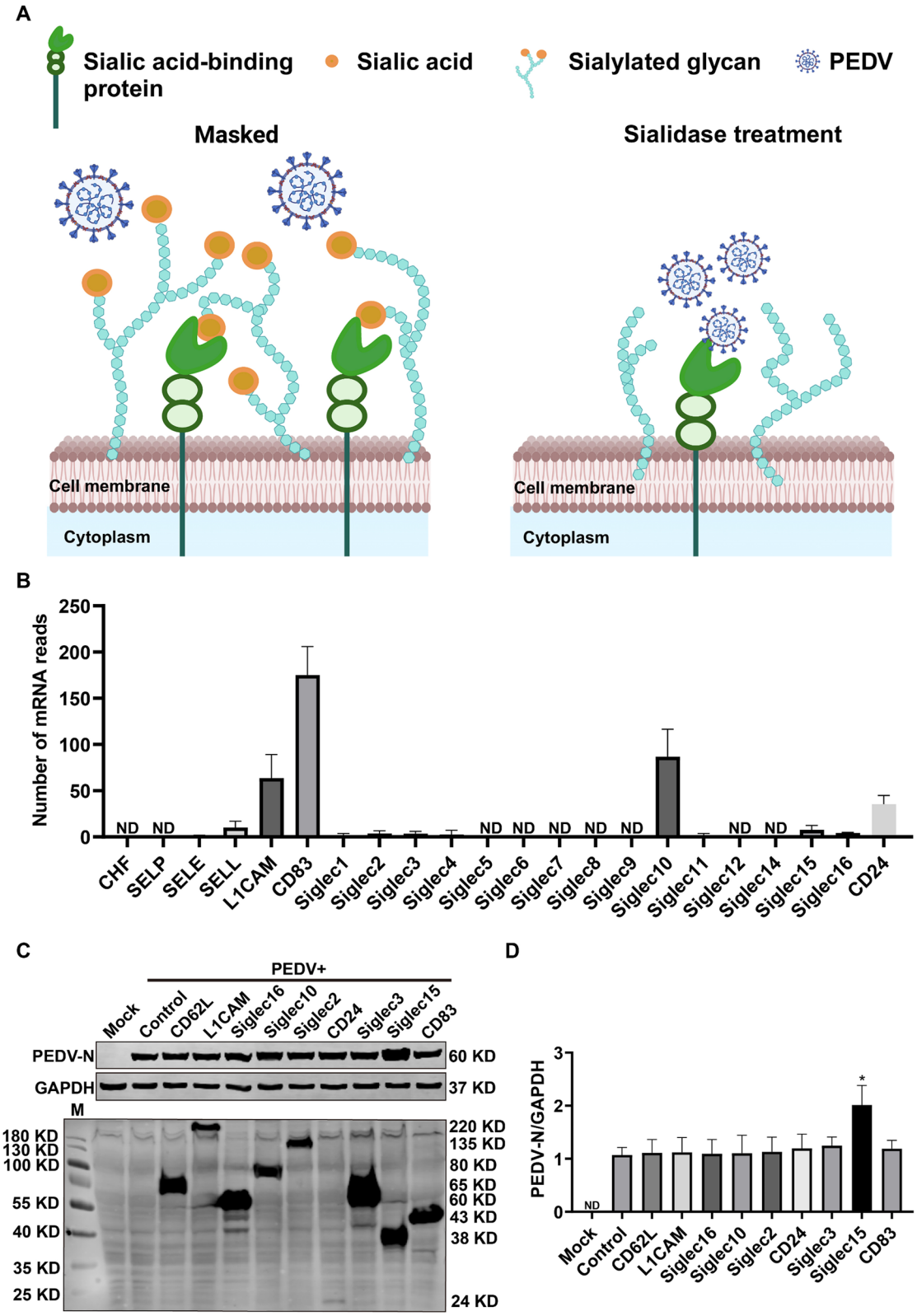

with a binding free energy (ΔiG) of −15.1 kcal/mol. The entropy change after dissociation (TΔS) was 13.1 kcal/mol.

We cotransfected plasmids expressing the light chain (pFUSE2-CLIg-rk1-IL2SP-26H4) and heavy chain (pFUSE2-CHIg-rG1-IL2SP-26H4) of the human Siglec-15

Fig. 2 Overexpression of Siglec-15 enhances PEDV infection (**A**) In the natural state, sialic acid-binding proteins are masked on the cell surface by sialic acid, which may hinder PEDV infection. However treatment with sialidase exposes sialic acid-binding proteins on the cell surface, potentially enhancing PEDV infection. (**B**) The expression of sialic acid-binding proteins in 293T cells was assessed via RNA-Seq. (**C**) The effects of overexpressing CD62L (75 kDa), L1CAM (160–220 kDa), Siglec-16 (60 kDa), Siglec-10 (80 kDa), CD22 (135 kDa), CD24 (25 kDa), CD33 (65 kDa), Siglec-15 (38 kDa), and CD83 (43 kDa) on PEDV infection in 293T cells were evaluated through Western blotting ($n=3$). (**D**) The expression of the PEDV N protein relative to that of GAPDH in **C** was quantified via ImageJ. The data are expressed as the means ± standard deviations and were analyzed via unpaired *t*-tests; $^{*}P<0.05$

monoclonal antibody into Expi293F cells. The culture supernatants were collected and enriched with Protein A Resin FF to obtain the human Siglec-15 monoclonal antibody (Fig. 8C). Western blot and immunofluorescence analyses demonstrated that the Siglec-15 monoclonal antibody could bind to Siglec-15 from humans, pigs, and mice (Fig. 8D-E). Additionally, the antibody effectively inhibited PEDV infection by approximately 80% in vitro (Fig. 8F). To confirm the blocking effect of the antibody in vivo, we utilized wild-type mice, *Siglec-15* knockout mice, and *Siglec-15* humanized mice as infection models. The results from RT-qPCR and immunohistochemistry indicated that the antibody effectively inhibited PEDV infection in the lungs of these mice (Fig. 8G-H). Thus, we developed a Siglec-15 monoclonal antibody that may be used for the treatment of PEDV infection in the future.

Discussion

PEDV is one of the major pathogens responsible for porcine diarrhea, and the infection rate remains high on pig farms. PEDV can also present as a mixed infection alongside other pathogens such as transmissible gastroenteritis virus (TGEV) and porcine deltacoronavirus (PDCoV) [61]. In addition to its sensitivity to porcine cells, PEDV has been shown to infect human HEK293T cells, mouse L929 cells, and green monkey Vero cells [62]. These findings indicate that PEDV possesses potential cross-species transmission capabilities, particularly its pronounced sensitivity to human cells, raising concerns about its possible transmission to humans.

The initiation of coronavirus infections is typically mediated by the spike protein and various cell surface receptors. Although PEDV has been studied since the 1970s, the specific receptor responsible for mediating its infection has not yet been identified. While porcine aminopeptidase N (pAPN) was initially proposed as a PEDV receptor, the susceptibility of pAPN knockout pigs to PEDV infection has led to its exclusion as a primary receptor [33]. In addition to pAPN, other factors implicated in the PEDV infection process include TfR1, Occludin, SLC35A1, EGFR, FSTL1, TLR4, and CNOT2 [35–40, 63]. But, these proteins are thought to be host factors or coreceptors rather than receptors. Sialic acid (SA) (N-acetylneuraminic acid (Neu5Ac)) can bind to the spike (S) protein of PEDV and has been suggested to act as a coreceptor for PEDV infection [26]. However, the binding of SA does not always promote coronavirus infection; instead, it can also inhibit infection, such as in the case of feline coronavirus (FECV), since sialidase treatments can lead to increased FECV infection [64]. Consistent with this observation, our data also demonstrated the inhibitory role of sialic acid in PEDV infection. We postulated that sialic acid on the cell surface might block virus and host receptor interactions by binding with PEDV or masking the receptor protein(s).

Interestingly, previous studies have shown that sialic acids on the cell surface can interact with and mask sialic acid-binding proteins, thereby inhibiting their ability to bind to ligands [49]. Our data demonstrated that the treatment of cells with sialidase can enhance PEDV infection, suggesting that sialic acid digestion may lead to the exposure of sialic acid-binding glycoproteins on the cell surface, which is consistent with our postulation that sialic acid-binding proteins may play an important role in PEDV infection. In particular, the digestion of sialic acid by sialidase may expose Siglec-15 on the cell surface for PEDV infection. Typically, Siglec-15 is expressed primarily on macrophages and dendritic cells within the spleen and lymph nodes, where it is involved in regulating osteoclast differentiation [56, 65]. Notably, Siglec-15 is also upregulated in human cancer cells and tumor-infiltrating myeloid cells, indicating its potential as a target for cancer immunotherapy [59]. While Siglec-15 has been implicated in the regulation of pulmonary infections caused by *Aspergillus* and *Streptococcus* [65], our present studies reveal its novel role in viral infections.

The binding of the coronavirus S protein to cell surface receptors is a crucial step in the initiation of infection [41]. As a member of the alpha coronavirus family, PEDV utilizes its S protein to interact with cell surface receptors during infection [7]. Our results indicate that Siglec-15 binds PEDV particles through interactions with the S and M proteins of the virus. Siglec-15 contains two core domains, the V-set and C2-set, with the V-set domain primarily responsible for ligand binding [49]. Interestingly, our results demonstrate that both the V-set and C2-set of Siglec-15 are involved in its binding to the S and M proteins. It is widely accepted that the CTD of the S1 subunit of coronaviruses, particularly the RBD, plays a critical role in viral infection [66]. However, our data indicate that the binding of the S1 subunit of PEDV to Siglec-15 primarily occurs within the amino acid range of 297–416 rather than within the CTD

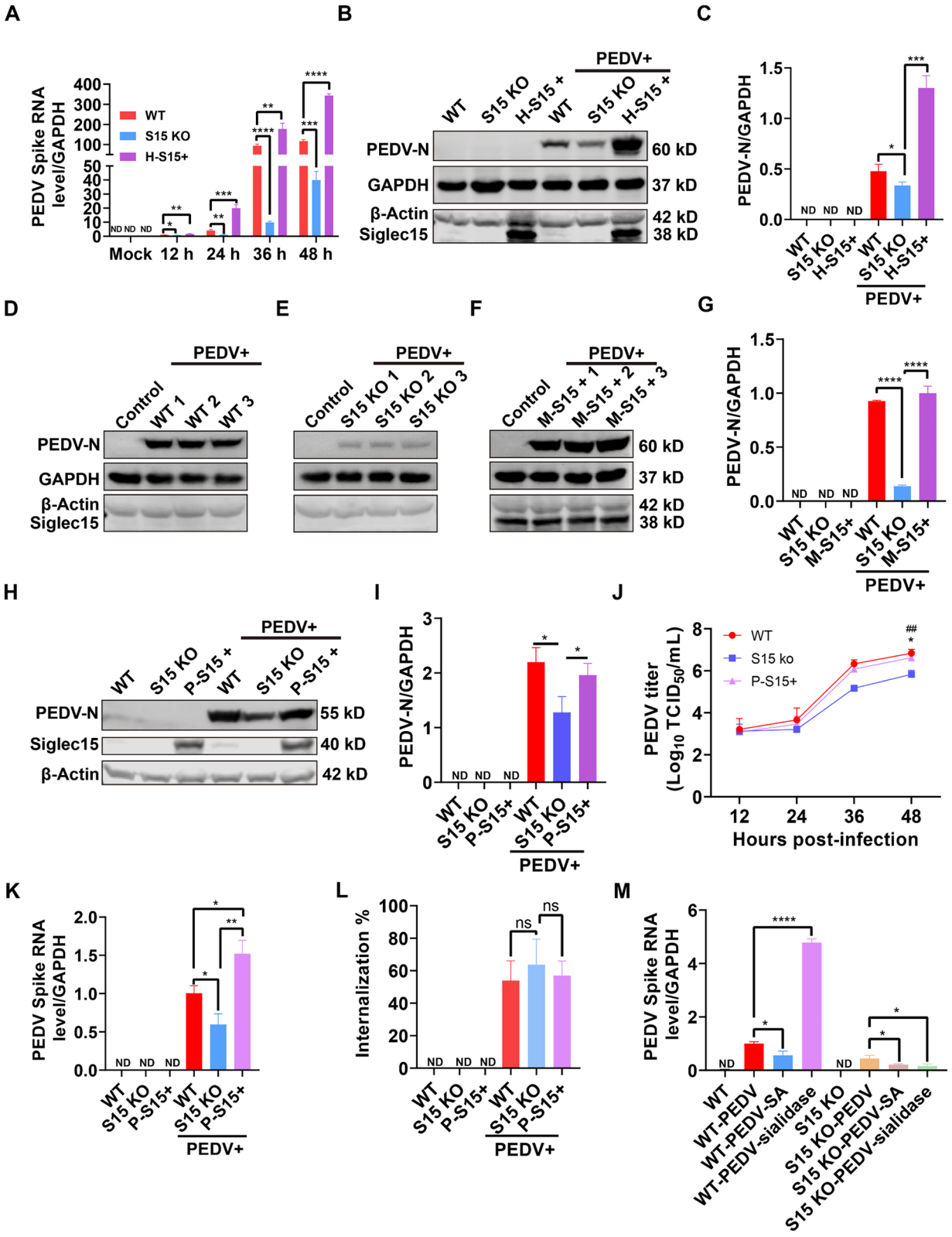

(509–638 aa) [26]. Previous studies have shown that the binding regions of the SARS-CoV-2 S protein with various receptors, such as ACE2, NRP-1, and CD147, are not exclusively located within the RBD [67, 68]. Therefore, the S protein of PEDV may possess distinct binding regions for different receptors. The above data need further structural

Fig. 3 Overexpression of Siglec-15 promotes PEDV infection by facilitating cellular adsorption (**A**) RT-qPCR results showing PEDV proliferation in 293T, 293T$^{Siglec-15-/-}$ or 293T$^{Siglec-15-/-}$-H-Siglec-15 cells at different time points (12 hpi, 24 hpi, 36 hpi, 48 hpi, 0.5 TCID50 (per cell)) of infection (n=3). (**B**) Western blotting results show the effects of *Siglec-15* knockout or overexpression in 293T cells on PEDV infection (0.5 TCID50 (per cell), 36 hpi) (n=3). (**C**) ImageJ was used to quantify the expression level of the PEDV N protein relative to that of GAPDH, as shown in **B**. (**D-F**) Western blotting was employed to assess the effects of *Siglec-15* knockout or overexpression in L929 cells on PEDV infection (0.5 TCID50 per cell, 36 hpi). (**G**) Quantification of the level of the PEDV N protein relative to that of GAPDH in (**D-F**) was performed via ImageJ. (**H**) Western blotting results illustrate the effects of Siglec-15 knockout and overexpression in LLC-PK1 cells on PEDV infection (1 TCID50 per cell, 36 hpi) (n=3). (**I**) The quantification of the PEDV N protein relative to that of GAPDH in (**D-F**) was also conducted via ImageJ. (**J**) The titers of PEDV in LLC-PK1, LLC-PK1$^{Siglec-15-/-}$ and LLC-PK1$^{Siglec-15-/-}$-P-Siglec-15 cells at different time points of infection (12 hpi, 24 hpi, 36 hpi, 48 hpi) were determined via the Spearman-Kärber method in Vero cells (*: P-S15+vs. S15 KO, #: WT vs. S15 KO) (n=3). (**K**) RT-qPCR was used to evaluate the effects of *Siglec-15* knockout and overexpression on PEDV adsorption (10 TCID50 per cell, maintained at 4 °C for 2 h) in LLC-PK1 cells (n=3). (**L**) The effects of *Siglec-15* knockout and overexpression on PEDV internalization in LLC-PK1 cells were determined by RT-qPCR (n=3). (**M**) RT-qPCR results demonstrating the effects of sialic acid and sialidase on PEDV adsorption in LLC-PK1, LLC-PK1$^{Siglec-15-/-}$ and LLC-PK1$^{Siglec-15-/-}$-P-Siglec-15 cells (n=3). The data are expressed as the means ± standard deviations and were analyzed via unpaired t-tests or two-way analysis of variance (ANOVA), *P<0.05, **P<0.01, ##P<0.01, ***P<0.001. S15 KO denotes Siglec-15 knockout cells; H-S15+indicates the rescue of human Siglec-15 expression in Siglec-15 knockout cells; M-S15+indicates the rescue of mouse Siglec-15 expression in Siglec-15 knockout cells; and P-S15+indicates the rescue of porcine Siglec-15 expression in Siglec-15 knockout cells

verification. Nevertheless, our data strongly support that Siglec-15 may function as a receptor by binding with the S protein to affect PEDV infection.

Our data also revealed an unexpected interaction between Siglec-15 and the M protein. In general, the coronavirus M protein plays a crucial role in viral particle assembly and evasion of the innate immune response [31]. The size of the M protein is significantly smaller than that of the S protein (10–20 nm) and no direct evidence of M protein protrusion size on the surface of the coronavirus has been reported [69]. Therefore, the binding of the M protein and Siglec-15 is likely to occur within the cell membrane after PEDV enters host cells. The significance of this interaction remains to be further explored.

Activation of the PI3K/Akt and Ras/ERK pathways has been shown to promote PEDV infection [70, 71]. Notably, Siglec-15 binds to the natural killer-activating receptor protein DAP12, which regulates the activation of spleen tyrosine kinase (Syk) [56]. Syk can either inhibit or activate downstream signaling pathways in different cell types. The phosphorylation of Syk leads to the activation of several downstream signaling pathways, including the PI3K/Akt [72], Ras/ERK [73], and IKK/NF-κB pathways [74]. Therefore, the interaction between the S (or M) protein and Siglec-15 may also be involved in regulating the Siglec-15-DAP12-SYK pathway during PEDV infection, and may indirectly influence the host cell and PEDV cross reaction, and their life trajectory.

The transmission routes of PEDV include fecal-oral and airborne pathways, which primarily target the intestine and respiratory tract [75]. The infection patterns of PEDV in mice resemble those in pigs, resulting in intestinal villus atrophy and epithelial cell shedding. However, in mice, Siglec-15 knockout significantly reduced PEDV infection and alleviated tissue damage caused by the virus. These findings suggest that Siglec-15 could be a promising target for the treatment of PEDV infection. Pigs are the natural hosts of PEDV; however, the virus is also capable of infecting cells from humans, mice, monkeys, and bats [26]. This cross-species sensitivity underscores the potential risk of PEDV transmission between species. Currently, PEDV infection is primarily managed through vaccination. However, the emergence of virulent strains (GIIs) has led to the reduced efficacy of traditional vaccines, highlighting the urgent need for the development of new vaccines or therapeutics to prevent or treat PEDV infections.

Antibody-based therapies have proven effective in treating both cancer and infectious diseases [76, 77]. Here, we successfully developed a monoclonal antibody that targets Siglec-15. This antibody effectively binds to Siglec-15 and inhibits PEDV infection both in vivo and in vitro. The predicted binding sites include Q163 and R166 of Siglec-15, which are also involved in the binding of the S1 subunit. On the basis of these findings, we propose that blocking the interaction between Siglec-15 and PEDV could be a promising strategy for treating PEDV infection.

In summary, the present study identified Siglec-15 as a key cellular receptor involved in PEDV infection. Furthermore, both in vivo and in vitro experiments demonstrated that the Siglec-15 antibody we developed can significantly inhibit PEDV infection, suggesting that Siglec-15 represents a promising target for therapeutic interventions. Our data set a cornerstone for further mechanistic studies underlying PEDV infection and provide new insights into future therapeutic development in dealing with challenges associated with PEDV infection.

Materials and methods

Cell lines, viruses, antibodies, and magnetic beads

Human embryonic kidney (HEK) 293T cells, L929 cells, Vero cells, LLC-PK1 cells, Expi293F cells, and IPEC-J2

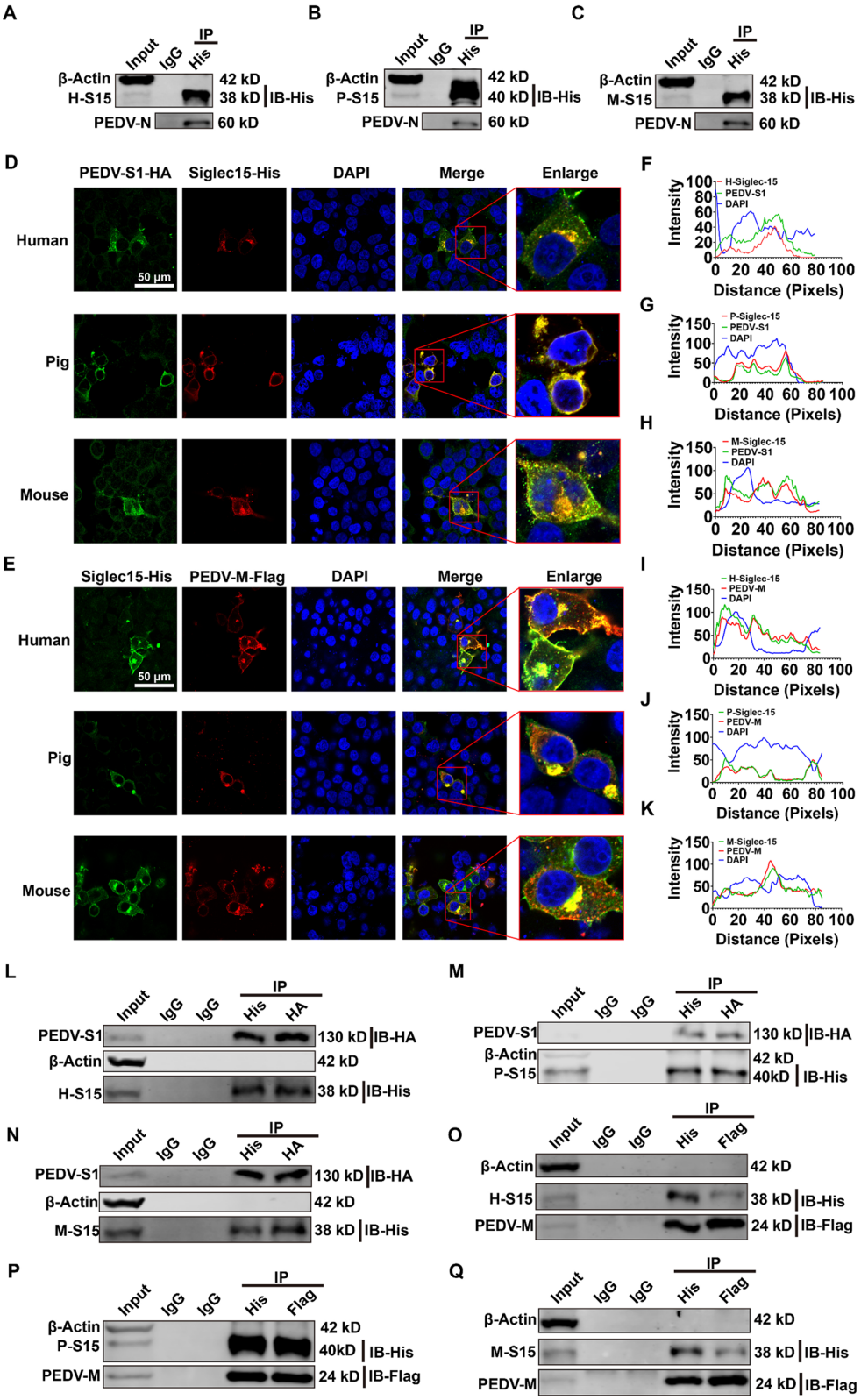

Fig. 4 Binding of Siglec-15 to PEDV particles mediated by S and M proteins. (**A**-**C**) Coimmunoprecipitation experiments demonstrated that Siglec-15 from humans, pigs, and mice can bind to PEDV particles. (**D**) Immunofluorescence analysis revealed the colocalization of human, pig, and mouse Siglec-15 with the S1 subunit in 293T cells. (**E**) Colocalization of human, pig, and mouse Siglec-15 with the M protein was confirmed in 293T cells through immunofluorescence. (**F**-**K**) Fluorescence colocalization analysis of the enlarged images in (**D**-**E**) was performed via ImageJ and GraphPad Prism. (**L**-**N**) Coimmunoprecipitation results indicate that Siglec-15 from humans, pigs, and mice can bind to the S1 subunit. (**O**-**Q**) Coimmunoprecipitation studies confirmed that Siglec-15 in humans, pigs, and mice can bind to the M protein. The scale bar in (**D**-**E**) indicates 50 μm

cells were obtained from the American Type Culture Collection (Manassas, VA, USA). All cells, except Expi293F cells, were cultured in Dulbecco's modified Eagle's medium (DMEM) (Cytiva, Shanghai, China) supplemented with 10% (v/v) fetal bovine serum (FBS) (Gibco, Grand Island, NY, USA), 10 μg/mL streptomycin, and 100 U/mL penicillin (BasalMedia, Shanghai, China). The cultures were maintained at 37 °C in a 5% CO_2 atmosphere. Expi293F cells were cultured in OPM-293-CD05 medium (81075, OPM, Shanghai, China) at 37 °C with 8% CO_2 and shaken at 120 rpm. The PEDV strain CHFJFQ (GenBank: OP688373.1) was isolated in our laboratory in 2018 from intestinal samples of pigs with diarrhea in Fuqing, Fujian, China.

The anti-PEDV N protein monoclonal antibodies anti-PEDV NP-FITC (SD-2 F-1) and anti-PEDV NP (SD-2-1) were purchased from Medgene Labs (Brookings, SD, USA). GAPDH monoclonal antibody (60004-1-Ig), beta-actin monoclonal antibody (81115-1-RR), His-tag polyclonal antibody (10001-0-AP), His-tag monoclonal antibody (66005-1-Ig), HA-tag polyclonal antibody (51064-2-AP), DYKDDDDK-tag polyclonal antibody (20543-1-AP), and Siglec-15 polyclonal antibody (28594-1-AP) were obtained from Proteintech Biotechnology Co., Ltd. (Wuhan, China). Additionally, IRDye® 800CW donkey anti-mouse or anti-rabbit IgG secondary antibodies (LI-COR, Lincoln, NE, USA), as well as Alexa Fluor 555 donkey anti-rabbit IgG (H+L) and Alexa Fluor 488 donkey anti-mouse IgG (H+L) highly cross-adsorbed secondary antibodies (Beyotime, Shanghai, China), were utilized. For coimmunoprecipitation assays, Mouse IgG (A7028, Beyotime, Shanghai, China), BeyoMag™ Protein G magnetic beads (P2105-1 mL, Beyotime, Shanghai, China), BeyoMag™ Anti-Flag Magnetic Beads (P2115-0.5 mL, Beyotime, Shanghai, China), BeyoMag™ Anti-His Magnetic Beads (P2135-0.5 mL, Beyotime, Shanghai, China) and BeyoMag™ Anti-HA Magnetic Beads (P2121-0.5 mL, Beyotime, Shanghai, China) were used.

Plasmids and SgRNA design

The overexpression plasmids for CD62L, L1CAM, Siglec-16, Siglec-10, Siglec-2, CD24, Siglec-3, Siglec-15, and CD83 (PLVX-CD62L, PLVX-L1CAM, PLVX-Siglec-16, PLVX-Siglec-10, PLVX-Siglec-2, PLVX-CD24, PLVX-Siglec-3, PLVX-Siglec-15 and PLVX-CD83) were synthesized by Tsingke Biotechnology Co., Ltd. (Beijing, China). Plasmids for expressing human, porcine, and mouse Siglec-15 (pLVX-H-Siglec-15-His, pLVX-P-Siglec-15-His, pLVX-M-Siglec-15-His), as well as vectors for expressing truncated forms of human and porcine Siglec-15 (pCDNA3.1-H-Siglec-15 (20–263 aa)-Fc, pLVX-P-S15ΔNRC-V-His, pLVX-P-S15ΔNRC-C2-His, pLVX-P-S15ΔV-C2-His), and vectors for the light and heavy chains of human Siglec-15 monoclonal antibodies (pFUSE2-CLIg-rk1-IL2SP-26H4, pFUSE2-CHIg-rG1-IL2SP-26H4) were synthesized by Beijing Tsingke Biotech Co., Ltd. (Beijing, China). The plasmid vectors used to overexpress the PEDV S1, S2, E, M, and N proteins (pLVX-S1-HA, pLVX-S2-HA, pLVX-E-Flag, pLVX-M-Flag, pLVX-N-Flag) were synthesized by Fuzhou Shangya Biotechnology Co., Ltd. (Fuzhou, China). The helper plasmids pCMV-VSV-G (#8454) and pSPAX2 for packaging lentivirus (#12260), the plasmid pX459 (#48139) for Siglec-15 knockout and the plasmid expressing TEV protease (pET28-MBP-super TEV protease) (#171782) were obtained from Addgene (Boston, MA, USA).

The sgRNA used for gene knockout was designed via the website http://www.e-crisp.org/ (sgRNA sequences are provided in Supplementary Table 1). Following annealing, the sgRNA was ligated with the BpiI-digested pX459 plasmid via T4 DNA ligase (2011 A, Takara, Tokyo, Japan). All plasmids were transformed into Trans1-T1 phage-resistant chemically competent cells (CD501-02, TransGen, Beijing, China) and cultured in Luria-Bertani (LB) media (10 g/L tryptone, 5 g/L yeast extract, and 10 g/L NaCl). A FastPure EndoFree Plasmid Mini Plus Kit (DC204-01, Vazyme, Nanjing, China) was utilized to extract the plasmids.

PEDV amplification and titer assays

PEDV was propagated in Vero cells, and the culture supernatant and cells were harvested when the cytopathic effect exceeded 80%. The supernatant was centrifuged at 3000 rpm for 5 minutes for titer determination. To investigate the effects of sialic acid and sialidase on PEDV proliferation, 1×10^6 cells (per well) and PEDV (1×10^6 TCID50 or 2×10^5 TCID50), along with various concentrations of sialic acid (1 mM, 0.5 mM, 0.25 mM, 0.125 mM) (S20140-5 g, Yuanye, Shanghai, China) or sialidase (0.01 U/mL, 0.02 U/mL, 0.03 U/mL, 0.04 U/mL) (S10170-25U, Yuanye, Shanghai, China), were added to each well of a 6-well plate. The cells were harvested at 36 h post-infection (hpi) for RNA or protein extraction, and PEDV proliferation was assessed via RT-qPCR or Western blot analysis.

293T cells were seeded at 1×10^6 cells per well in 6-well plates and cultured for 12 h. Cells were then transfected with overexpression plasmids using Lipofectamine™ 3000 (L3000-008, Invitrogen, Carlsbad, CA, USA) according to the manufacturer's instructions. The following plasmids were used for transfection: pLVX-CD62L, pLVX-L1CAM, pLVX-Siglec-16, pLVX-Siglec-10, pLVX-Siglec-2, pLVX-CD24, pLVX-Siglec-3, pLVX-Siglec-15, and pLVX-CD83. Control cells were transfected with the empty vector pLVX-E. At 12 h post-transfection, 1×10^6 cells per well were

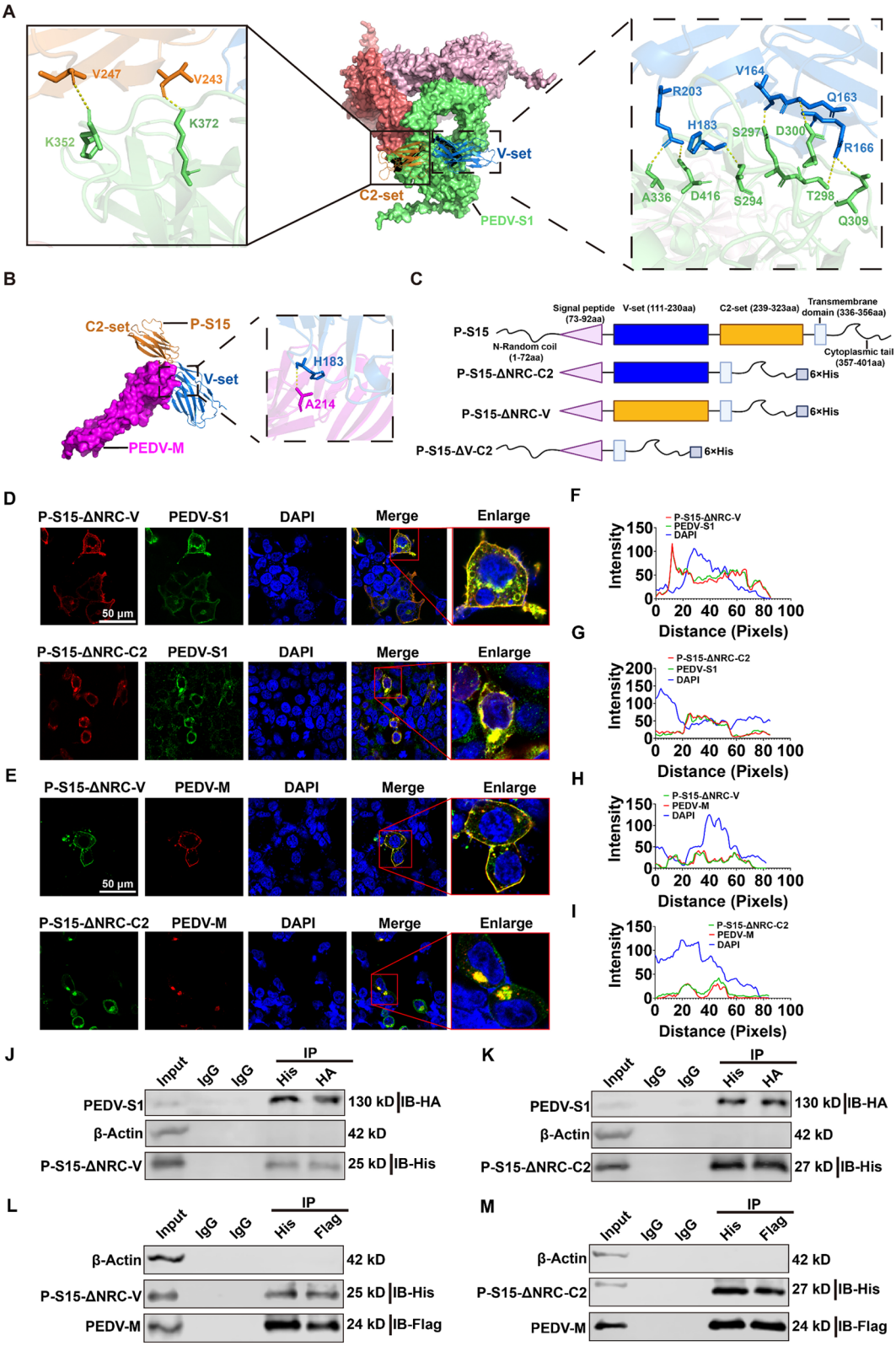

seeded in 6-well plates and infected with PEDV (MOI = 0.1) for 36 h. Subsequently, Western blot analyses were performed to assess the expression of the PEDV N protein and determine the impact of CD62L, L1CAM, Siglec-16, Siglec-10, Siglec-2, CD24, Siglec-3, Siglec-15, and CD83 overexpression on PEDV infection.

Fig. 5 The V-set and C2-set domains of Siglec-15 are involved in its binding to the PEDV S1 subunit and M protein. (**A**) 3D structure prediction and molecular docking of Siglec-15 and the S1 subunit were performed via AlphaFold 3 (Lime pink, Deep Salmon; and green represents the trimer of the S1 subunit, blue represents the V-set of Siglec-15, and orange represents the C2-set of Siglec-15). The interaction between Siglec-15 and the S1 subunit was analyzed via PDBePISA and PyMOL software. The binding sites on Siglec-15 include residues Q163, V164, R166, H183, R203, V243, and V247, whereas the binding sites on the S1 subunit include S294, S297, D300, Q309, A336, K352, K372 and D416. (**B**) Similarly, 3D structure prediction and molecular docking between Siglec-15 and the M protein were conducted via AlphaFold 3, with magenta representing the M protein, blue representing the V-set of Siglec-15, and orange representing the C2-set of Siglec-15. The interaction characteristics of Siglec-15 with the M protein were analyzed via PDBePISA and PyMOL software. The binding site on Siglec-15 was identified as H183, whereas the binding site on the M protein was located at A214. (**C**) A schematic diagram illustrating the full-length and truncated forms of pig Siglec-15. (**D**) Coexpression of the PEDV S1 subunit with either P-S15ΔNRC-V or P-S15ΔNRC-C2 in 293T cells was assessed by immunofluorescence to detect colocalization with the S1 subunit. (**E**) Immunofluorescence analysis confirmed the colocalization of P-S15ΔNRC-V or P-S15ΔNRC-C2 with the M protein in 293T cells. (**F**-**I**) Fluorescence colocalization analysis of the enlarged images in (**D**-**E**) was performed via ImageJ and GraphPad Prism. (**J**-**K**) Coimmunoprecipitation results indicate that P-S15ΔNRC-V or P-S15ΔNRC-C2 can bind to the S1 subunit. (**L**-**M**) The binding of P-S15ΔNRC-V or P-S15ΔNRC-C2 to the M protein was further confirmed through coimmunoprecipitation assays. The scale bar in (**D**-**E**) indicates 50 μm

PEDV was propagated in LLC-PK1, LLC-PK1$^{Siglec-15-/-}$, and LLC-PK1$^{Siglec-15-/-}$-P-S15 cells. A total of 1×10^6 cells (per well) were added to a 6-well plate for coculture with 1×10^6 TCID50 or 1×10^5 TCID50 of PEDV (per well). The culture supernatant was collected every 12 h for titer determination. The virus titer was assessed via the Spearman-Kärber method [78, 79].

PEDV adsorption and internalization assays

To investigate the effects of sialic acid and sialidase on PEDV cell adsorption, 293T cells were cultured in confocal dishes (2×10^5 cells/dish) or 6-well plates (1×10^6 cells/well) for 12 h. PEDV (1×10^7 TCID50 in 1 mL) was treated with sialic acid (1 mM) at 37 °C for 2 h, added to [79] were incubated with sialidase (0.04 U/mL) at 37 °C for 2 h. The culture media were then discarded, and the cells were incubated with 1×10^7 TCID50 of PEDV at 4 °C for 2 h. Afterward, the cells were washed twice with PBS (4 °C), and fixed with 4% paraformaldehyde (1 mL) at room temperature for 1 h, and PEDV cell adsorption was assessed by immunofluorescence. RNA was extracted from the cells in the 6-well plates via TRIzol™, and the cell adsorption of PEDV was subsequently assessed via RT-qPCR.

To explore the effects of Siglec-15 on PEDV adsorption and internalization, 1×10^6 LLC-PK1, LLC-PK1$^{Siglec-15-/-}$, or LLC-PK1$^{Siglec-15-/-}$-P-S15 cells were added to each well of a 6-well plate and cultured for 12 h. After the culture medium was discarded, 1×10^7 TCID50 of PEDV was added to each well, and the samples were incubated at 4 °C for 2 h. The cells were then washed three times with PBS. For internalization analysis, after PEDV adsorption, 2 mL of DMEM was added, and the cells were incubated at 37 °C for 2 h. A citric acid solution (pH = 3) consisting of 23.93 g/L sodium citrate dihydrate and 3.52 g citric acid was used to wash the cells three times. Following PEDV adsorption or internalization, the efficiency of adsorption and internalization was evaluated via RT-qPCR or immunofluorescence.

RNA sequencing and data processing

RNA was extracted from 1×10^7 293T cells per sample, with three biological replicates, for RNA sequencing. Total RNA was extracted via TRIzol™ reagent (Sigma-Aldrich) following the manufacturer's instructions. A total of 2 μg of RNA was used as the starting material for RNA sample preparation. The sequencing libraries were constructed via the NEBNext Ultra™ RNA Library Preparation Kit (New England BioLabs, USA) according to the manufacturer's guidelines. Index-labeled samples were clustered on the cBot Cluster Generation System via the TruSeq PE Cluster Kit v3-cBot-HS (Illumina, Inc.). After cluster generation, the libraries were sequenced on the Illumina NovaSeq platform, which produced paired-end reads. Library construction and Illumina sequencing were performed by WUHAN IGENEBOOK BIOTECHNOLOGY CO., LTD. (Wuhan, China). Clean reads were obtained by removing adapter sequences, poly-N stretches, and low-quality reads from the raw data. The quality of the clean data was assessed by calculating the Q20, Q30, and GC contents, and sequence duplication levels. Clean reads were aligned to the reference genome (GRCh38.p14) via HISAT2 (v.2.2.1), and gene expression levels for each sample were quantified with featureCounts (v.2.0.6).

Construction of stable *Siglec-15*-overexpressing and *Siglec-15*-knockout cell lines

The pLVX-H-Siglec-15, pCMV-VSV-G, and pSPAX2 plasmids (8:4:6) μg were transfected into 293T cells (100 mm petri dish, approximately 85% confluence) via Lipofectamine™ 3000 to package the lentivirus. 5×10^5 293T$^{Siglec-15-/-}$ cells were added to each well of a 6-well plate and cocultured with 1 mL of lentiviruses for 36 h. The Siglec-15 stable transgenic 293T cells were selected with puromycin (A1113803, Gibco, Grand Island, NY, USA) at a final concentration of 2 μg/mL.

For knockout experiments, 5×10^5 cells (293T, L929, or LLC-PK1) were plated in each well of a 6-well plate for

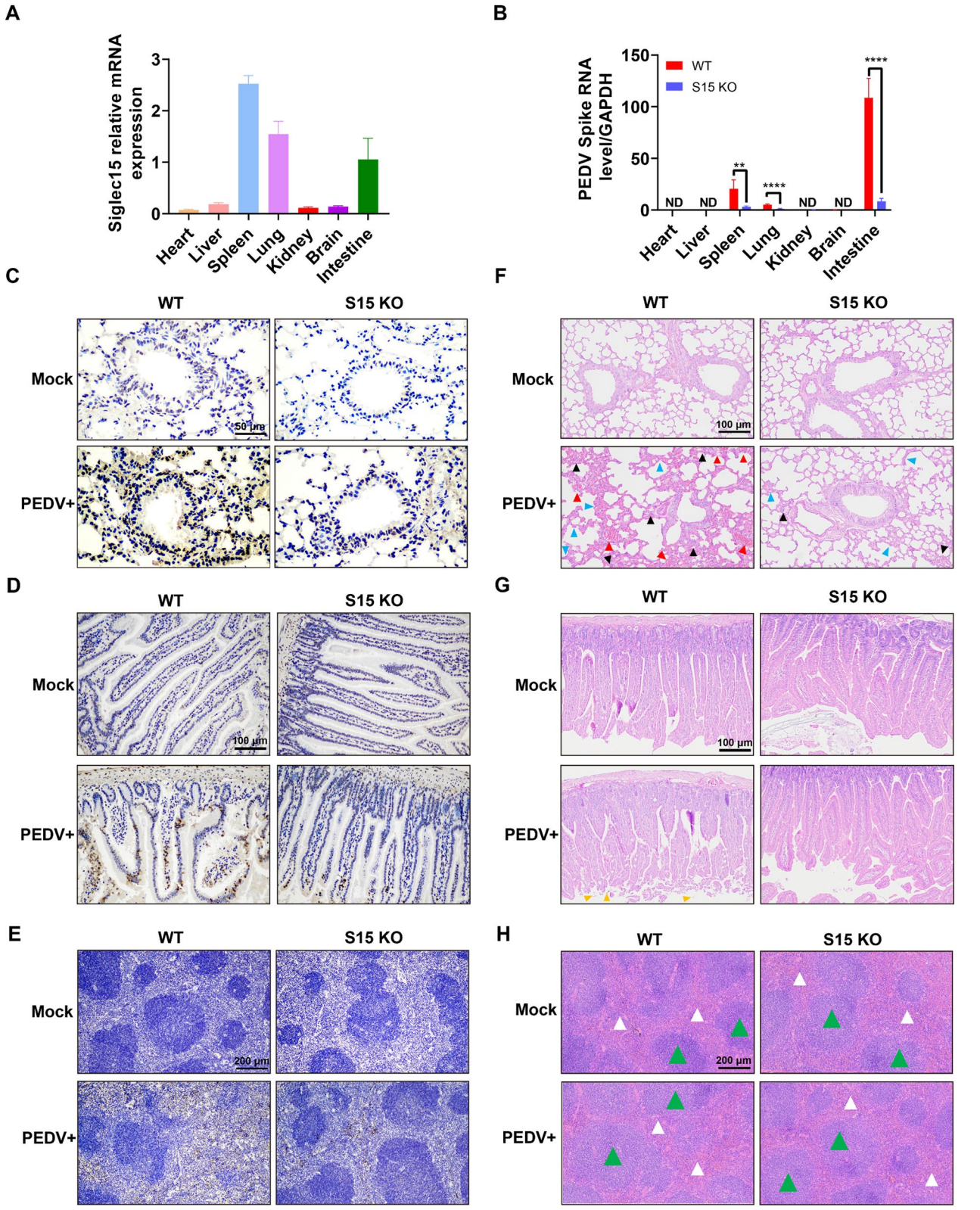

12 h. Each well was transfected with 4 μg of the knockout plasmid via Lipofectamine™ 3000, cultured for 36 h and selected with puromycin for 3 days (293T: 2 μg/mL, L929: 7 μg/mL, LLC-PK1: 4 μg/mL). The surviving cells were used to isolate monoclonal cells.

Fig. 6 Siglec-15 knockout reduces PEDV infection and alleviates lung and intestinal tissue damage in mice. (**A**) RT-qPCR was utilized to measure the expression levels of Siglec-15 in the heart, liver, spleen, lung, kidney, brain, and small intestine of the mice ($n=5$). (**B**) The levels of PEDV infection (1×10^6 TCID50, 72 hpi) in the heart, liver, spleen, lung, kidney, brain, and small intestine were assessed in both wild-type and *Siglec-15* knockout mice via RT-qPCR ($n=5$). (**C-E**) Immunohistochemical staining was conducted to detect PEDV infection in the lungs, small intestines, and spleens of wild-type and Siglec-15 knockout mice. (**F**) H&E staining revealed lung damage due to PEDV infection, including hemorrhage (red triangle), inflammation (black triangle), and thickening of the alveolar walls (blue triangle). (**G**) H&E staining highlighted the shedding of epithelial cells from the small intestinal villi resulting from PEDV infection (yellow arrow). (**H**) H&E staining revealed distinct areas of red pulp (green triangle) and white pulp (white triangle) within the spleen. The data are expressed as the means ± standard deviations and were analyzed via two-way analysis of variance (ANOVA), $^{**}P<0.01$, $^{****}P<0.0001$. The scale bars represent 50 μm in **C**, 100 μm in **D** and (**F-G**), and 200 μm in **E** and **H**

Genomic DNA was extracted via the FastPure Cell/Tissue DNA Isolation Mini Kit (DC102-01, Vazyme, Nanjing, China). One hundred nanograms of DNA were used for PCR to amplify the target fragment of *Siglec-15* (the PCR primers are listed in Supplementary Table 2). Siglec-15 gene knockout was confirmed by sequencing analyses conducted by Beijing Tsingke Biotech Co., Ltd. (Beijing, China), and the sequences were analyzed via BioEdit software (v.7.0.5.3).

Western blotting

Proteins were extracted via RIPA buffer (P0013B, Beyotime, Shanghai, China), and their concentrations were determined via the Enhanced BCA Protein Assay Kit (P0010, Beyotime, Shanghai, China). Sixty micrograms of protein were loaded for SDS-polyacrylamide gel electrophoresis, and the proteins were transferred to a polyvinylidene difluoride (PVDF) membrane (IPFL00010, Millipore, Massachusetts, USA). The PVDF membrane was blocked with a 5% bovine serum albumin (BSA) solution (V900933, Sigma-Aldrich, St. Louis, MO, USA) at room temperature for 2 h. Primary antibodies, including GAPDH (1:5000), β-actin (1:5000), anti-PEDV NP (1:1000), Siglec-15 (1:1000), His (1:500), Flag (1:500), and HA (1:500), were incubated with the samples at 4 °C for 12 h. Next, the sections were incubated with IRDye® 800CW donkey anti-mouse IgG secondary antibody (1:10,000) and IRDye® 800CW donkey anti-rabbit IgG secondary antibody (1:10,000) at room temperature for 2 h. The PVDF membrane was then visualized via a LI-COR Odyssey infrared fluorescence scanner (LI-COR) after washing with TBST. The primary antibodies were diluted in 5% BSA, while the secondary antibodies were diluted in TBST.

Reverse transcription-quantitative polymerase chain reaction (RT-qPCR)

Total RNA from cells and tissues was extracted via TRIzol™ (15596018; Thermo Fisher, Waltham, MA, USA). cDNA was synthesized from 1 μg of RNA via HiScript® III RT SuperMix for qPCR (+gDNA wiper) (R323-01, Vazyme, Nanjing, China). The qPCR mixture consisted of 100 ng of cDNA (2 μL), forward and reverse primers (0.5 μL each at 100 μM), 10 μL of ChamQ Universal SYBR qPCR Master Mix (Q711-02/03, Vazyme, Nanjing, China), and 7 μL of ddH2O. The reactions were incubated at 95 °C for 10 min, followed by 40 cycles of 95 °C for 10 s and 60 °C for 30 s. GAPDH was used as the normalization control. The mRNA levels are presented as fold changes relative to those in the control group and were calculated via the $2^{-\Delta\Delta Ct}$ method. The expression stability of each gene was verified by averaging triplicate Ct values (RT-qPCR primers are listed in Supplementary Table 3).

Flow cytometry

One million 293T, 293T$^{Siglec-15-/-}$, or 293T$^{Siglec-15-/-}$-H-S15 cells were added to each well of a 6-well plate and cocultured with 5×10^5 TCID50 of PEDV per well. The cells were digested with 0.25% trypsin and harvested every 12 h. For fixation and permeabilization, the cells were treated with 1 mL of fixation/permeabilization solution (554714, BD Biosciences, Franklin Lakes, NJ, USA) at room temperature for 15 min. Following centrifugation at 400 × g for 5 minutes, the supernatant was discarded, and 1 mL of ddH_2O-diluted Perm/Wash™ Buffer (554714, BD Biosciences, Franklin Lakes, NJ, USA) was added and incubated for 10 min at room temperature. Next, 1 × Perm/Wash™ Buffer and 1 μL of anti-PEDV NP-FITC (SD-2 F-1, Medgene Labs, Brookings, SD, USA) were added and incubated at room temperature for 2 h. After another centrifugation at 400 × g for 5 minutes, the supernatant was discarded, and the cells were resuspended in 1 mL of PBS containing 1% FBS. The samples were analyzed via a FACSymphony™ A5 cell analyzer (BD Biosciences, Franklin Lakes, NJ, USA), and the data were processed via FlowJo software (v.10.8).

Immunofluorescence and coimmunoprecipitation

HEK293T cells (5×10^6 cells per dish) were cultured in a 100 mm diameter dish for 12 h. The plasmids pLVX-H-Siglec-15-His, pLVX-P-Siglec-15-His, and pLVX-M-Siglec-15-His, which are designed to overexpress human, pig, and mouse Siglec-15, or the plasmids pLVX-P-S15ΔNRC-V-His, pLVX-P-S15ΔNRC-C2-His, and pLVX-P-S15ΔV-C2-His for overexpressing truncated forms of

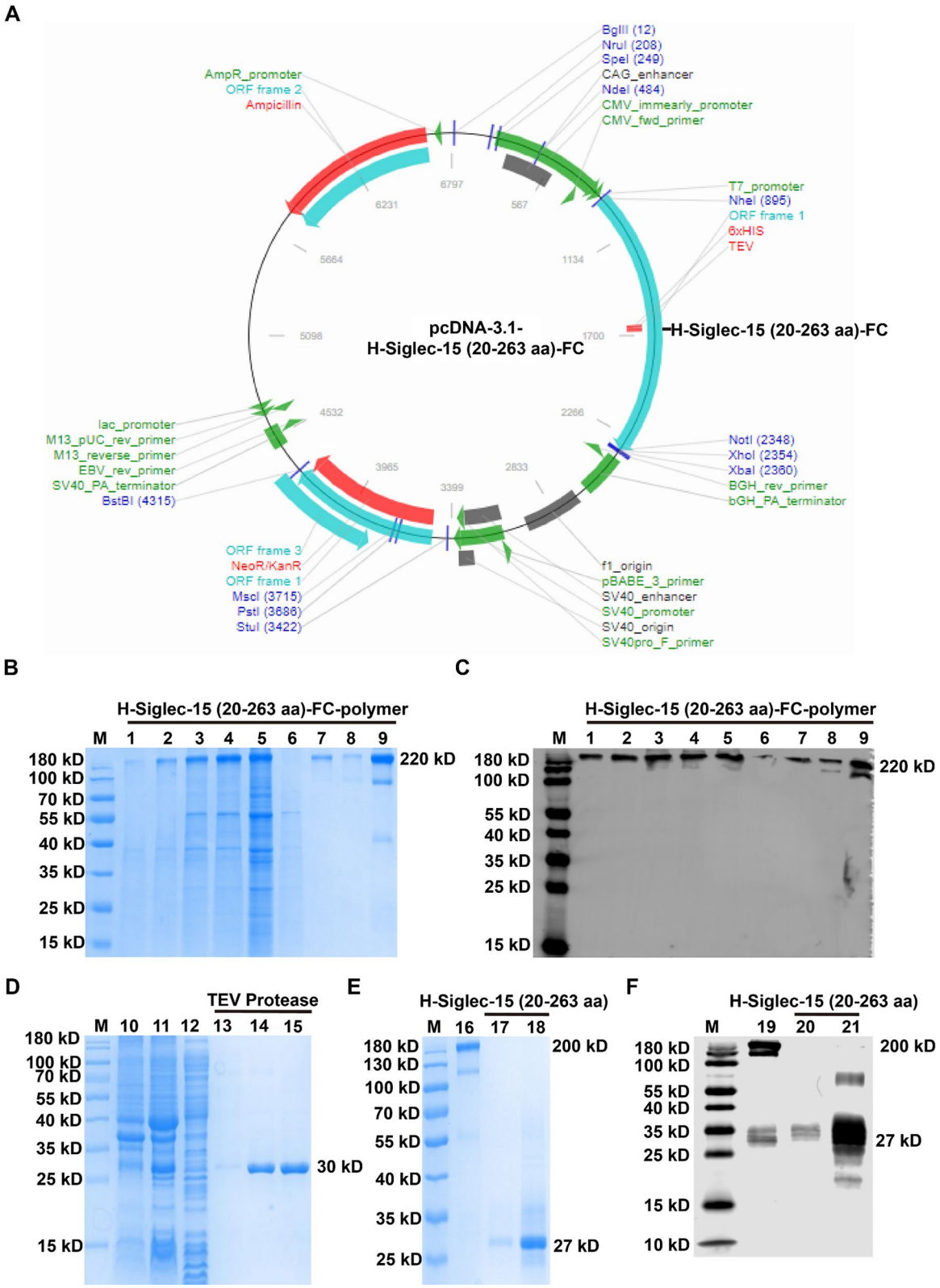

porcine Siglec-15, were cotransfected into the 293T cells via Lipofectamine™ 3000 along with the plasmids pLVX-S1-HA and pLVX-M-Flag, which overexpress the PEDV S1 and M proteins, respectively. At 36 h posttransfection, 2×10^5 cells were cultured in confocal dishes for an additional 12 h, followed by washing with phosphate-buffered

Fig. 7 Expression and purification of H-Siglec-15 (20-263aa). (**A**) Schematic representation of the plasmids used for the expression of H-Siglec-15 (20-263aa)-Fc. (**B**) The expression of H-Siglec-15 (20-263aa)-Fc (approximately 220 kDa) in the culture supernatant of Expi293F cells was analyzed by SDS-PAGE and Coomassie blue staining. Samples 1–4 represent the culture supernatants collected on the third, fourth, fifth, and sixth days posttransfection, respectively. Sample 5 included the culture supernatant and cell precipitate from the sixth day, whereas samples 6 and 7 included the flow-through and elution of H-Siglec-15 (20-263aa)-Fc, respectively. Sample 8 was the cleaning solution, and sample 9 was the protein concentrate. M denotes the molecular weight marker. (**C**) Western blot analysis of H-Siglec-15 (20-263aa)-Fc expression in the culture supernatant of Expi293F cells. Samples 1–9 correspond to the same samples as in **B**, with M indicating the molecular weight marker. (**D**) The expression of TEV protease (approximately 30 kDa) was detected by SDS-PAGE and Coomassie blue staining. Samples 10 and 11 represent the precipitate and supernatant following cell lysis, whereas samples 12, 13, 14, and 15 represent the flow-through and elution at 20 mM, 80 mM, and 200 mM imidazole, respectively. M denotes the molecular weight marker. (**E**) Cleavage of the H-Siglec-15 (20-263aa)-Fc protein by the TEV protease was analyzed via SDS-PAGE and Coomassie blue staining. Sample 16 contains the uncleaved H-Siglec-15 (20-263aa)-Fc protein (220 kDa), whereas sample 17 contains the cleaved H-Siglec-15 (20-263aa) protein (approximately 27 kDa). Sample 18 was the concentrated cleaved H-Siglec-15 (20-263aa) protein. M denotes the molecular weight marker. (**F**) Cleavage of the H-Siglec-15 (20-263aa)-Fc protein by the TEV protease was confirmed by Western blot analysis. Samples 19–21 correspond to the same samples as in **E**, with M indicating the molecular weight marker

saline (PBS). The cells were then fixed at room temperature for 30 min with 1 mL of immunostaining fix solution (P0098-500 mL, Beyotime, Shanghai, China). The cells were subsequently permeabilized with 1 mL of immunostaining permeabilization buffer containing Triton X-100 (P0096-500 mL; Beyotime, Shanghai, China) for 15 min at room temperature and blocked with QuickBlock™ Blocking Buffer for immunostaining (P0260, Beyotime, Shanghai, China) for 15 min at room temperature.

Primary antibodies (His (1:200) with Flag (1:200) or His (1:200) with HA (1:200)) were added and incubated at 4 °C for 12 h. The cells were then washed twice with PBS, and Alexa Fluor 555 Donkey anti-rabbit IgG (H+L) and Alexa Fluor 488 Donkey anti-mouse IgG (H+L), both highly cross-adsorbed secondary antibodies (1:500), were added and incubated at room temperature for 2 h. After two additional washes with PBS, 200 μL of 2-(4-amidinophenyl)-6-indolecarbamidine dihydrochloride (DAPI) (C1005, Beyotime, Shanghai, China) was added, and the mixture was incubated at room temperature for 10 min. Imaging was performed via an LSM 780 laser confocal system (Zeiss, Oberkochen, Germany).

At 36 h posttransfection, the cells were harvested for protein extraction via RIPA buffer. Magnetic beads (20 μL) were added and incubated for 12 h at 4 °C. The magnetic beads were then separated via a DynaMag-2 magnet (Thermo Fisher Scientific, Waltham, MA, USA), and the beads were washed twice with TBST. Subsequently, 40 μL of RIPA buffer and 10 μL of SDS-PAGE loading buffer (5×) (P0015L, Beyotime, Shanghai, China) were added, and the mixture was heated at 95 °C for 5 min. The supernatant was collected for Western blot analysis.

For the coimmunoprecipitation experiment involving PEDV virus particles and Siglec-15, magnetic beads were coated with Siglec-15 and then incubated with PEDV (1×10^8 TCID50) at 4 °C for 12 h. The binding of Siglec-15 to PEDV was subsequently detected by Western blot analysis.

Hematoxylin-eosin (H&E) staining and immunohistochemistry

The mice were infected with PEDV, and tissues (heart, liver, spleen, lung, kidney, brain, and small intestine) were fixed in 4% paraformaldehyde at room temperature for 12 h. For hematoxylin-eosin (H&E) staining, the tissues were dehydrated in ethanol, embedded in paraffin, and sectioned at a thickness of 4 μm. These sections were dewaxed, made transparent, and stained with hematoxylin and eosin to evaluate histopathological changes. For immunohistochemistry, paraffin sections were dewaxed and rehydrated, and tissue antigens were retrieved at high temperatures and pressure. The samples were treated with 3% H_2O_2, followed by blocking with 10% BSA at room temperature for 2 h. The primary antibody (anti-PEDV NP at a dilution of 1:400) was added, and the samples were incubated at 4 °C for 12 h. Subsequently, 100 μL of horseradish peroxidase (HRP)-conjugated goat anti-mouse IgG (1:5000) (A0216, Beyotime, Shanghai, China) was added, and the mixture was incubated at 37 °C for 2 h. Finally, PEDV infection was observed via DAB staining with hematoxylin counterstaining.

Expression and purification of the TEV protease

A plasmid (pET28-MBP-super TEV protease) expressing TEV protease was transfected into competent BL21 (DE3) cells (Thermo Fisher Scientific, Waltham, MA, USA). Positive clones were selected by screening with kanamycin sulfate (K8020; SOLARBIO, Beijing, China). These positive clones were cultured in an LB medium and induced with 1 mol/L isopropyl-β-D-thiogalactopyranoside (IPTG) (I1020, SOLARBIO, Beijing, China) to express TEV protease. The TEV protease was purified via a nickel column and eluted with 200 mM imidazole.

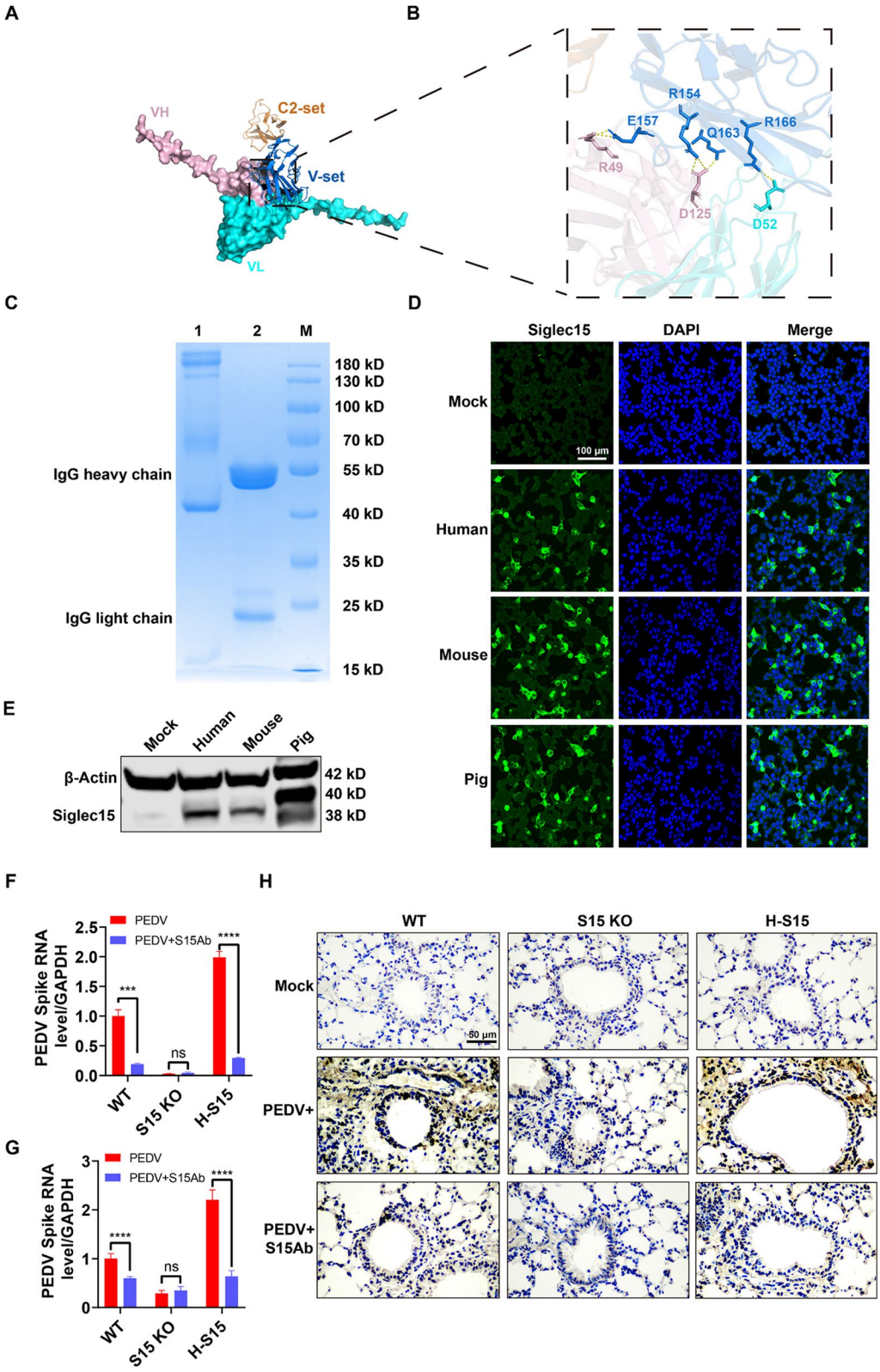

H-Siglec-15 (20–263 aa) purification and immunization

Five hundred micrograms of plasmid (pCDNA3.1-H-Siglec-15 (20-263aa)-Fc) were transfected into Expi293F cells (cell density of 3×10^6 cells/mL in 200 mL) via

Fig. 8 Siglec-15 monoclonal antibody effectively blocks PEDV infection. (**A**) 3D structure prediction and molecular docking of the Siglec-15 and Siglec-15 monoclonal antibodies (VH and VL domains) were performed via AlphaFold 3 (light pink and cyan represent the Siglec-15 monoclonal antibody VH and VL domains, respectively). Blue represents the V-set of Siglec-15, and orange represents the C2-set of Siglec-15). (**B**) The interaction between Siglec-15 and Siglec-15 monoclonal antibodies was analyzed via PDBePISA and PyMOL software. The binding sites on Siglec-15 include residues R154, E157, Q163, and R166, whereas the binding sites on the Siglec-15 monoclonal antibody include VH-CDR1 (R49), VH-CDR3 (D125), and VL-CDR1 (D52). (**C**) The expression of the Siglec-15 monoclonal antibody was analyzed by SDS-PAGE and Coomassie blue staining. Sample 1 was prepared with a loading buffer without β-ME, while Sample 2 contained a loading buffer with β-ME. M indicates the molecular weight marker. (**D-E**) Human, mouse, and pig Siglec-15 were overexpressed in 293T cells. The binding capacity of the prepared Siglec-15 monoclonal antibody was assessed via immunofluorescence and Western blotting. (**F**) RT-qPCR was used to evaluate the blocking effect of the Siglec-15 monoclonal antibody on PEDV infection in 293T, $293T^{Siglec-15-/-}$ and $293T^{Siglec-15-/-}$-H-Siglec-15 cells ($n=3$). (**G-H**) The blocking effect of the Siglec-15 monoclonal antibody on PEDV infection in the lungs of wild-type, *Siglec-15* knockout, and Siglec-15-humanized mice was assessed via RT-qPCR and immunohistochemistry (1×10^6 TCID50, 72 hpi, $n=5$). The data are expressed as the means ± standard deviations and were analyzed via two-way analysis of variance (ANOVA), ***$P<0.001$, ****$P<0.0001$. The scale bars in **B** and **F** represent 100 μm and 50 μm, respectively

polyethylenimine. Following transfection, the culture was maintained for 7 days, after which the supernatant was collected. The protein was enriched via Protein A Resin FF (L00464, GenScript, Nanjing, China) and eluted with a glycine solution (0.1 M). The protein was then concentrated in a 30 kDa ultrafiltration tube. H-Siglec-15 (20-263aa)-Fc was digested with TEV protease, and the Fc fragment, along with the TEV protease, was removed via a Protein A Resin FF and a nickel column. A total of 1.5 mL of H-Siglec-15 (20-263aa) (1 mg/mL) was mixed with 1.5 mL of Freund's complete adjuvant (F5881, Sigma-Aldrich, St. Louis, MO, USA) and emulsified for immunization of a 3-month-old New Zealand rabbit. Immunization was performed every two weeks for a total of three immunizations.

H-Siglec-15 monoclonal antibody Preparation

The rabbits were immunized three times with H-Siglec-15 (20–263 aa), and venous blood was collected to extract B cells. The light and heavy chains (VL and VH) of the Siglec-15 antibodies were obtained through nested PCR and ligated to the expression plasmid (nested PCR primers are listed in Supplementary Table 4). Both the light and heavy chains (VL and VH) were double-digested with EcoRI and Eco91I and then linked via T4 DNA ligase. Plasmids expressing the human Siglec-15 monoclonal antibody light chain (pFUSE2-CLIg-rk1-IL2SP-26H4) and heavy chain (pFUSE2-CHIg-rG1-IL2SP-26H4) were cotransfected into Expi293F cells. After 6 days of culture, the antibodies were enriched with Protein A Resin FF (L00464; GenScript, Nanjing, China). Finally, the antibodies were eluted with a glycine solution (0.1 M) and concentrated in a 30 kDa ultrafiltration tube.

PEDV infection in mice

Six-week-old C57BL/6J wild-type mice and Siglec-15 knockout mice were divided into a control group and a PEDV inoculation group, with 5 mice in each group. The mice in the inoculation group received 1×10^6 TCID50 of PEDV (100 μL) *via* gavage, while those in the control group were administered DMEM. The experiment was terminated at 72 h post-infection (hpi). RT-qPCR and immunohistochemistry were used to detect PEDV infection in the organs of the mice, and H&E staining was used to assess tissue damage caused by PEDV infection. Specific pathogen-free C57BL/6J male mice (6 weeks old) were randomly allocated to the experimental groups and maintained at the Animal Experimental Center of Fujian Normal University under controlled conditions of 23–25 °C, 40–60% humidity, and a 12 h light/dark cycle, with free access to food. C57BL/6J wild-type mice were obtained from Wu's Animal Center (Fuzhou, China), while C57BL/6J-Siglec15 knockout mice were obtained from Cyagen Biosciences Inc. (Guangzhou, China).

Siglec-15 antibody blockage of PEDV infection in cells and mice

One million 293T, $293T^{Siglec-15-/-}$, or $293T^{Siglec-15-/-}$-H-S15 cells were added to each well of a 6-well plate. After 12 h of culture, 10 μg (20 μL) of the Siglec-15 monoclonal antibody was added (the control group received an equal volume of PBS) and incubated at 37 °C for 30 min. The culture medium was then replaced with fresh medium, and 5×10^5 TCID50 (per well) of PEDV was added, followed by continuing culture for 2 h. The culture media was then replaced with fresh media, followed by continued culture for 36 h. RT-qPCR was employed to assess the blocking effect of the Siglec-15 monoclonal antibody on PEDV infection.

Six-week-old wild-type mice, Siglec-15 knockout mice, and Siglec-15 humanized mice were divided into a control group, a PEDV inoculation group, and a Siglec-15 antibody blocking group, with 5 mice in each group. The PEDV inoculation group received an intranasal inoculation of 1×10^6 TCID50 (50 μL) of PEDV, whereas both the PEDV inoculation group and the Siglec-15 antibody blocking group were treated with 50 μL of DMEM and 50 μg of Siglec-15 antibody *via* nasal drip 30 min prior to PEDV inoculation. The experiment was terminated at 72 h post-infection (hpi), and the lungs of the mice were collected for detection of

PEDV infection via RT-qPCR and immunohistochemistry. C57BL/6J-Siglec15 humanized mice were obtained from GemPharmatech Co., Ltd. (Jiangsu, China).

Prediction and analysis of protein interaction structure

The amino acid sequences of the S1 and M proteins of PEDV and porcine Siglec-15 were obtained from the National Center for Biotechnology Information (NCBI) (https://www.ncbi.nlm.nih.gov/), with the following protein IDs: Siglec-15 (XP_003121465.3, https://www.ncbi.nlm.nih.gov/protein/1191806540), PEDV-CHFJFQ S (WFG70067.1, https://www.ncbi.nlm.nih.gov/protein/2476855545), and PEDV-CHFJFQ M (WFG70070.1, https://www.ncbi.nlm.nih.gov/protein/2476855548). The 3D complex of porcine Siglec-15 with the PEDV S1 or M proteins was simulated via molecular docking *via* AlphaFold3 (https://www.alphafoldserver.com) [80], with the molar ratios of Siglec-15 to PEDV S1 and M proteins set at 1:3 and 1:1, respectively. Protein-protein interactions were analyzed via PDBePISA (v.1.52) [81], which provides thermodynamic properties of the complexes, including binding free energy (ΔiG), entropy change after dissociation (TΔS), and the interface area (Å²). Amino acid residues involved in interactions between protein complexes were analyzed via the PDBsum (v.2.2) online tool (https://www.ebi.ac.uk/pdbsum) [82]. Finally, the complex structure was visualized via PyMOL (v.3.0) [83].

Statistical analyses

Image processing was conducted via Adobe Illustrator 2022, BioEdit (v.7.0.5.3), and ImageJ (v.1.8.0). Statistical analyses were performed with GraphPad Prism (v.8.0), employing unpaired *t*-tests and two-way analyses of variance (ANOVAs). The results are presented as the means ± standard deviations (SDs), with significance set at $P < 0.05$.

Supplementary Information The online version contains supplementary material available at https://doi.org/10.1007/s00018-025-05672-2.

Author contributions Zhihua Feng, writing - review & editing, writing - original draft, visualization, validation, supervision, software, resources, methodology, investigation, formal analysis, data curation, conceptualization. Yajuan Fu, writing - original draft, visualization, methodology, investigation, data curation. Sheng Yang, Visualization, methodology, investigation, formal analysis. Heng Zhao, visualization, methodology, investigation, formal analysis. Minhua Lin, Visualization, methodology, investigation, formal analysis. Chuancheng Liu, visualization, methodology, investigation, formal analysis. Weili Huang, Visualization, methodology, investigation, formal analysis. Xinyan He, visualization, methodology, investigation, formal analysis. Yao Chen, visualization, methodology, investigation, formal analysis. Jianxin Chen, formal analysis, funding acquisition. Yangkun Shen, writing - review & editing, supervision, project administration, funding acquisition, conceptualization. Zhaolong Li, writing - review & editing, supervision, project administration, conceptualization. Qi Chen, conceptualization, research planning, supervision, writing - review & editing, validation, project administration, funding acquisition.

Funding This work was supported by the National Natural Science Foundation of China (Grant Nos. 82350126 and 82171991), and the Natural Science Foundation of Fujian Province, China (Grant No. 2022J01652).

Data availability The data supporting the findings of this study are openly available in the article and can be obtained from the corresponding author upon request. Raw sequencing data and processed count data for RNA sequencing supporting the findings of this study have been deposited in the National Center for Biotechnology Information's Gene Expression Omnibus and are accessible through GEO series accession number: https://www.ncbi.nlm.nih.gov/geo/query/acc.cgi? acc=GSE284990.

Declarations

Ethics approval and consent to participate The experiments were approved by the Institutional Animal Care and Use Committee of Fujian Normal University and Fujian Medical University (Approval Nos. IACUC-20220039 and FJMU IACUC-2018079). All experiments were performed in accordance with the Guide for the Care and Use of Laboratory Animals.

Competing interests The research was conducted in the absence of any commercial or financial relationships.

Open Access This article is licensed under a Creative Commons Attribution-NonCommercial-NoDerivatives 4.0 International License, which permits any non-commercial use, sharing, distribution and reproduction in any medium or format, as long as you give appropriate credit to the original author(s) and the source, provide a link to the Creative Commons licence, and indicate if you modified the licensed material. You do not have permission under this licence to share adapted material derived from this article or parts of it. The images or other third party material in this article are included in the article's Creative Commons licence, unless indicated otherwise in a credit line to the material. If material is not included in the article's Creative Commons licence and your intended use is not permitted by statutory regulation or exceeds the permitted use, you will need to obtain permission directly from the copyright holder. To view a copy of this licence, visit http://creativecommons.org/licenses/by-nc-nd/4.0/.

References

1. Qiao WT et al (2024) Matrine exhibits antiviral activities against PEDV by directly targeting Spike protein of the virus and inducing apoptosis via the MAPK signaling pathway. Int J Biol Macromol 270:132408
2. Wang Q et al (2024) ACADM inhibits AMPK activation to modulate PEDV-induced lipophagy and β-oxidation for impairing viral replication. J Biol Chem 300:107549
3. Jung K, Saif LJ, Wang Q (2020) Porcine epidemic diarrhea virus (PEDV): an update on etiology, transmission, pathogenesis, and prevention and control. Virus Res 286:198045
4. Sun RQ, Cai RJ, Chen YQ, Liang PS, Chen DK, Song CX (2012) Outbreak of Porcine epidemic diarrhea in suckling piglets, China. Emerg Infect Dis 18:161–163

5. Wen Z et al (2018) Oral administration of coated PEDV-loaded microspheres elicited PEDV-specific immunity in weaned piglets. Vaccine 36:6803–6809
6. Pensaert MB, de Bouck P (1978) A new coronavirus-like particle associated with diarrhea in swine. Arch Virol 58:243–247
7. Lin F et al (2022) Insights and advances into types, function, structure, and receptor recognition. Viruses 14:1744
8. Wang D, Fang L, Xiao S (2016) Porcine epidemic diarrhea in China. Virus Res 226:7–13
9. Li W et al (2012) New variants of Porcine epidemic diarrhea virus. China 2011 Emerg Infect Dis 18:1350–1353
10. Wang XM et al (2013) Genetic properties of endemic Chinese Porcine epidemic diarrhea virus strains isolated since 2010. Arch Virol 158:2487–2494
11. Boniotti MB et al (2018) Porcine epidemic diarrhoea virus in Italy: disease spread and the role of transportation. Transbound Emerg Dis 65:1935–1942
12. Huang YW et al (2013) Origin, evolution, and genotyping of emergent Porcine epidemic diarrhea virus strains in the united States. mBio 4:e00737–e00713
13. Kochhar HS, Canada (2014) Porcine epidemic diarrhea in Canada: an emerging disease case study. Can Veterinary J = La Revue Veterinaire Canadienne 55:1048–1049
14. Theuns S et al (2015) Complete genome sequence of a porcine epidemic diarrhea virus from a novel outbreak in belgium, january 2015. *Genome announcements* 3, e00506-15
15. Steinrigl A, Fernández SR, Stoiber F, Pikalo J, Sattler T, Schmoll F (2015) First detection, clinical presentation and phylogenetic characterization of Porcine epidemic diarrhea virus in Austria. BMC Vet Res 11:310
16. Zhang H et al (2023) Global dynamics of Porcine enteric coronavirus PEDV epidemiology, evolution, and transmission. Mol Biol Evol 40:msad052
17. Bi J, Zeng S, Xiao S, Chen H, Fang L (2012) Complete genome sequence of Porcine epidemic diarrhea virus strain AJ1102 isolated from a suckling piglet with acute diarrhea in China. J Virol 86:10910–10911
18. Wen Z et al (2018) Genetic epidemiology of Porcine epidemic diarrhoea virus Circulating in China in 2012–2017 based on Spike gene. Transbound Emerg Dis 65:883–889
19. Liang W et al (2020) Isolation and evolutionary analyses of Porcine epidemic diarrhea virus in Asia. PeerJ 8:e10114
20. Antas M, Woźniakowski G (2019) Current status of Porcine epidemic diarrhoea (PED) in European pigs. J Veterinary Res 63:465–470
21. Xu X et al (2023) The novel Nsp9-interacting host factor H2BE promotes PEDV replication by inhibiting Endoplasmic reticulum stress-mediated apoptosis. Vet Res 54:27
22. Yang X et al (2013) Genetic variation analysis of reemerging Porcine epidemic diarrhea virus prevailing in central China from 2010 to 2011. Virus Genes 46:337–344
23. Li Z, Ma Z, Li Y, Gao S, Xiao S (2020) Porcine epidemic diarrhea virus: molecular mechanisms of Attenuation and vaccines. Microb Pathog 149:104553
24. Li W, Wicht O, van Kuppeveld FJ, He Q, Rottier PJ, Bosch BJ (2015) A single point mutation creating a Furin cleavage site in the Spike protein renders Porcine epidemic diarrhea coronavirus trypsin independent for cell entry and fusion. J Virol 89:8077–8081
25. Wicht O et al (2014) Proteolytic activation of the Porcine epidemic diarrhea coronavirus Spike fusion protein by trypsin in cell culture. J Virol 88:7952–7961
26. Liu C et al (2015) Receptor usage and cell entry of Porcine epidemic diarrhea coronavirus. J Virol 89:6121–6125
27. Kirchdoerfer RN et al (2021) Structure and immune recognition of the porcine epidemic diarrhea virus spike protein. Structure (London, England: 1993) 29, 385–392.e385
28. Chen Y et al (2018) Porcine epidemic diarrhea virus S1 protein is the critical inducer of apoptosis. Virol J 15:170
29. Tan Y et al (2022) Correction for Tan Trypsin-Enhanced Infection with Porcine Epidemic Diarrhea Virus Is Determined by the S2 Subunit of the Spike Glycoprotein. *Journal of virology* 96, e0040522
30. Arndt AL, Larson BJ, Hogue BG (2010) A conserved domain in the coronavirus membrane protein tail is important for virus assembly. J Virol 84:11418–11428
31. de Haan CA, Vennema H, Rottier PJ (2000) Assembly of the coronavirus envelope: homotypic interactions between the M proteins. J Virol 74:4967–4978
32. Lu Y et al (2020) Virus-like particle vaccine with B-cell epitope from Porcine epidemic diarrhea virus (PEDV) incorporated into hepatitis B virus core capsid provides clinical alleviation against PEDV in neonatal piglets through lactogenic immunity. Vaccine 38:5212–5218
33. Shirato K et al (2016) Porcine aminopeptidase N is not a cellular receptor of Porcine epidemic diarrhea virus, but promotes its infectivity via aminopeptidase activity. J Gen Virol 97:2528–2539
34. Luo L et al (2019) Aminopeptidase N-null neonatal piglets are protected from transmissible gastroenteritis virus but not Porcine epidemic diarrhea virus. Sci Rep 9:13186
35. Zhang S, Cao Y, Yang Q (2020) Transferrin receptor 1 levels at the cell surface influence the susceptibility of newborn piglets to PEDV infection. PLoS Pathog 16:e1008682
36. Luo X et al (2017) Tight junction protein occludin is a Porcine epidemic diarrhea virus entry factor. J Virol 91:e00202–e00217
37. Wang J et al (2023) Genome-scale CRISPR screen identifies TRIM2 and SLC35A1 associated with Porcine epidemic diarrhoea virus infection. Int J Biol Macromol 250:125962
38. Liu C et al (2025) FSTL1 and TLR4 interact with PEDV structural proteins to promote virus adsorption to host cells. J Virol 99:e0183724
39. Zhang XZ, Tian WJ, Wang J, You JL, Wang XJ (2022) Death receptor DR5 as a proviral factor for viral entry and replication of coronavirus PEDV. Viruses 14:2724
40. Wang J et al (2022) CCR4-NOT complex 2-A cofactor in host cell for Porcine epidemic diarrhea virus infection. Genes 13:1504
41. Su Y, Hou Y, Wang Q (2019) The enhanced replication of an S-intact PEDV during coinfection with an S1 NTD-del PEDV in piglets. Vet Microbiol 228:202–212
42. Lübbers J, Rodríguez E, van Kooyk Y (2018) Modulation of immune tolerance via Siglec-Sialic acid interactions. Front Immunol 9:2807
43. Smith BAH, Bertozzi CR (2021) The clinical impact of glycobiology: targeting Selectins, Siglecs and mammalian glycans. Nat Rev Drug Discovery 20:217–243
44. Schmidt CQ, Hipgrave Ederveen AL, Harder MJ, Wuhrer M, Stehle T, Blaum BS (2018) Biophysical analysis of Sialic acid recognition by the complement regulator factor H. Glycobiology 28:765–773
45. Duan S, Paulson JC (2020) Siglecs as immune cell checkpoints in disease. Annu Rev Immunol 38:365–395
46. Kleene R, Yang H, Kutsche M, Schachner M (2001) The neural recognition molecule L1 is a Sialic acid-binding lectin for CD24, which induces promotion and Inhibition of neurite outgrowth. J Biol Chem 276:21656–21663
47. Wakitani S et al (2008) Effects of leukemia inhibitory factor on lectin-binding patterns in the uterine stromal vessels of mice. Immunobiology 213:143–150
48. Urano-Tashiro Y, Yajima A, Takahashi Y, Konishi K (2012) Streptococcus gordonii promotes rapid differentiation of monocytes

into dendritic cells through interaction with the Sialic acid-binding adhesin. Odontology 100:144–148
49. Crocker PR, Paulson JC, Varki A (2007) Siglecs and their roles in the immune system. Nat Rev Immunol 7:255–266
50. Chang YC, Nizet V (2020) Siglecs at the Host-Pathogen interface. Adv Exp Med Biol 1204:197–214
51. Duan X, Nauwynck HJ, Favoreel HW, Pensaert MB (1998) Identification of a putative receptor for Porcine reproductive and respiratory syndrome virus on Porcine alveolar macrophages. J Virol 72:4520–4523
52. Vanderheijden N et al (2003) Involvement of Sialoadhesin in entry of Porcine reproductive and respiratory syndrome virus into Porcine alveolar macrophages. J Virol 77:8207–8215
53. Sewald X et al (2015) Retroviruses use CD169-mediated trans-infection of permissive lymphocytes to Establish infection. Sci (New York NY) 350:563–567
54. Zou Z et al (2011) Siglecs facilitate HIV-1 infection of macrophages through adhesion with viral Sialic acids. PLoS ONE 6:e24559
55. Varchetta S et al (2013) Sialic acid-binding Ig-like lectin-7 interacts with HIV-1 gp120 and facilitates infection of CD4pos T cells and macrophages. Retrovirology 10:154
56. Angata T, Tabuchi Y, Nakamura K, Nakamura M (2007) Siglec-15: an immune system Siglec conserved throughout vertebrate evolution. Glycobiology 17:838–846
57. Ishida-Kitagawa N et al (2012) Siglec-15 protein regulates formation of functional osteoclasts in concert with DNAX-activating protein of 12 kda (DAP12). J Biol Chem 287:17493–17502
58. Jaeger M et al (2019) A systems genomics approach identifies SIGLEC15 as a susceptibility factor in recurrent vulvovaginal candidiasis. Sci Transl Med 11:eaar3558
59. Wang J et al (2019) Siglec-15 as an immune suppressor and potential target for normalization cancer immunotherapy. Nat Med 25:656–666
60. Hu J et al (2021) Siglec15 shapes a non-inflamed tumor microenvironment and predicts the molecular subtype in bladder cancer. Theranostics 11:3089–3108
61. Su M et al (2020) A molecular epidemiological investigation of PEDV in China: characterization of co-infection and genetic diversity of S1-based genes. Transbound Emerg Dis 67:1129–1140
62. Zhou J et al (2024) Unveiling the role of protein kinase C Θ in Porcine epidemic diarrhea virus replication: insights from Genome-Wide CRISPR/Cas9 library screening. Int J Mol Sci 25:3096
63. Zhang Y et al (2023) Porcine epidemic diarrhea virus causes diarrhea by activating EGFR to regulates NHE3 activity and mobility on plasma membrane. Front Microbiol 14:1237913
64. Desmarets LMB, Theuns S, Roukaerts IDM, Acar DD, Nauwynck HJ (2014) Role of Sialic acids in feline enteric coronavirus infections. J Gen Virol 95:1911–1918
65. Huang R, Zheng J, Shao Y, Zhu L, Yang T (2023) Siglec-15 as multifunctional molecule involved in osteoclast differentiation, cancer immunity and microbial infection. Prog Biophys Mol Biol 177:34–41
66. Deng F et al (2016) Identification and comparison of receptor binding characteristics of the Spike protein of two Porcine epidemic diarrhea virus strains. Viruses 8:55
67. Cantuti-Castelvetri L et al (2020) Neuropilin-1 facilitates SARS-CoV-2 cell entry and infectivity. Sci (New York NY) 370:856–860
68. Fenizia C et al (2021) SARS-CoV-2 entry: at the crossroads of CD147 and ACE2. Cells 10:1434
69. Wrapp D et al (2020) Cryo-EM structure of the 2019-nCoV Spike in the prefusion conformation. Sci (New York NY) 367:1260–1263
70. Lin H, Li B, Liu M, Zhou H, He K, Fan H (2020) Nonstructural protein 6 of Porcine epidemic diarrhea virus induces autophagy to promote viral replication via the PI3K/Akt/mTOR axis. Vet Microbiol 244:108684
71. Kim Y, Lee C (2015) Extracellular signal-regulated kinase (ERK) activation is required for Porcine epidemic diarrhea virus replication. Virology 484:181–193
72. Wang S et al (2022) TREM2 drives microglia response to amyloid-β via SYK-dependent and -independent pathways. Cell 185:4153–4169e4119
73. Parsa KV, Butchar JP, Rajaram MV, Cremer TJ, Tridandapani S (2008) The tyrosine kinase Syk promotes phagocytosis of Francisella through the activation of Erk. Mol Immunol 45:3012–3021
74. Oh J et al (2012) Syk/Src pathway-targeted inhibition of skin inflammatory responses by carnosic acid. Mediators of inflammation 781375
75. Li Y, Wu Q, Huang L, Yuan C, Wang J, Yang Q (2018) An alternative pathway of enteric PEDV dissemination from nasal cavity to intestinal mucosa in swine. Nat Commun 9:3811
76. Cao Y et al (2022) Omicron escapes the majority of existing SARS-CoV-2 neutralizing antibodies. Nature 602:657–663
77. Janjigian YY et al (2021) The KEYNOTE-811 trial of dual PD-1 and HER2 Blockade in HER2-positive gastric cancer. Nature 600:727–730
78. Spearman C (1908) The method of right and wrong cases (constant stimuli) without Gauss's formulae. Br J Psychol 2:227
79. Kärber G (1931) Beitrag Zur kollektiven behandlung Pharmakologischer Reihenversuche. Naunyn-Schmiedebergs Archiv Für Experimentelle Pathologie Und Pharmakologie 162:480–483
80. Abramson J et al (2024) Accurate structure prediction of biomolecular interactions with alphafold 3. Nature 630:493–500
81. Krissinel E, Henrick K (2007) Inference of macromolecular assemblies from crystalline state. J Mol Biol 372:774–797
82. Laskowski RA, Chistyakov VV, Thornton JM (2005) PDBsum more: new summaries and analyses of the known 3D structures of proteins and nucleic acids. Nucleic Acids Res 33:D266–268
83. Sanner MF, Olson AJ, Spehner JC (1996) Reduced surface: an efficient way to compute molecular surfaces. Biopolymers 38:305–320

Publisher's note Springer Nature remains neutral with regard to jurisdictional claims in published maps and institutional affiliations.